UNIVERSITY OF CALIFORNIA

Los Angeles

Translational regulation medicated by lncRNA Miat in cardiac hypertrophy

A dissertation submitted in partial satisfaction of the requirements
for the degree
Doctor of Philosophy
in
Molecular, Cellular and Integrative Physiology

by

He Wang
2020

ABSTRACT OF THE DISSERTATION

Translational regulation medicated by lncRNA Miat

in cardiac hypertrophy

by

He Wang

Doctor of Philosophy

In

Molecular, Cellular and Integrative Physiology

University of California, Los Angeles, 2020

Professor Yibin Wang, Chair

Elevated protein synthesis is a fundamental mechanism contributing to a growing heart, during which both translation efficiency and capacity are enhanced (6-8). Translation efficiency focus on existing ribosomes in the cytosol, involving how signaling pathways regulate translation initiation, elongation, termination and ribosome recycling to affect translation in a cell(9-12). In the cardiomyocytes, mRNA of MHC loading to the polysomes(15), phosphorylation of ribosomal protein, S6, or of the peptide chain initiation factor, elF-4E by mTOR (16) are well-characterized mechanisms of translation efficiency regulation. While little of translation capacity, or ribosome biogenesis in the heart has been explored. In the heart, ribosome biogenesis is vital in rapid growth conditions such as cardiac development, hypertrophy and pulmonary artery stenosis(7). The left ventricular weight increases 82% in 4 days following birth in the newborn pig(17) serves as a good example

illustrating that regulation of translation efficiency only cannot meet the demand of elevated protein synthesis.

Biogenesis of ribosomes, the only and universal translation machinery in the cell, is a tremendous work. All three RNA polymerases, estimated 70% of mature ribosomes and more than 200 assembly factors are devoted in this tightly controlled process(14, 18, 19). It starts from rDNA transcription, the pre-ribosomal RNA 45S/47S is synthesized by Pol I, followed by ribosomal RNA processing in the nucleoli, carried out by ~150 exonucleases, processing factors and ribosomal subunit assembly factors. The rRNA stands as a scaffold to be decorated by ribosomal proteins, then exported into the cytosol as the 40S and 60S subunits. In the heart, regulation of this assembly chain is largely dark as only few studies examined the rDNA transcription level.

In the thesis, we identified a long non-coding RNA Miat is associated with cardiac hypertrophy from an unbiased approach and analyzed the transcriptional change in the pressure overload mouse model to discover that Miat regulates the ribosomal genes and ribosome assembly associated genes. To confirm its impact on translation, we found that Miat is required for increased protein synthesis in cardiomyocytes. More remarkably, lack of Miat showed protective effect to the heart in multiple stress-induced cardiac growth models. Mechanistically, we found that Miat binds to nucleolin (NCL) via conserved binding motifs, and such binding is vital for ribosome biogenesis. NCL is a protein required for rDNA transcription and functions as the early processor of 45S/47S rRNA (1, 20, 21), however, how NCL mediates 45S/47S rRNA processing in the nucleoli region remained unknown. We found that Miat-NCL binding is vital for rRNA processing, nucleoli formation and ribosome biogenesis in

the cardiomyocytes. Therefore, our study provided one of the first detailed examples of how ribosome biogenesis is regulated in the heart and how alteration of translation capacity affects cardiac function in pathological growth.

The dissertation of He Wang is approved.

Reza Ardehali

Jau-nian Chen

Thomas Vondriska

Yibin Wang, Committee Chair

University of California, Los Angeles

2020

DEDICATION

To my parents, Shu-ye and Xiu-hui, for your unconditional and unlimited love;

To my little brother Zhong-zi, for the sunshine and humor you bring into my life;

To Josh, for your trust and love, especially when I don't even hold them to myself;

Last but not least,

To my dog JoJo, for you are the one spent the most time with me on this journey.

TABLE OF CONTENTS AND LISTS

LIST OF TABLES----- --- --- --- --- ------ --- --- --- --- ------ --- --- --- --- ------ --- - -- --- - -XI

LIST OF FIGURES----- --- --- --- --- ------ --- --- --- --- ----- --- --- --- --- --------- - -- --- ---XII

ACKNOWLEDGEMENTS --- --- --- --- --- ------ --- --- --- --- ------ --- --- --- --- --------- ---VII

BIBLIOGRAPHY---- --- --- --- --- ------ --- --- --- --- ------ --- --- --- --- ------ --- --------- ----IX

ABSTRACT----- --- --- --- --- ------ --- --- --- --- ------ --- --- --- --- ------ --- --- --- - ------ --- III

GLOSSARY---- --- --- --- --- ------ --- --- --- --- ------ --- --- --- --- ------ --- --- --- --- ---- ----XIII

TABLE OF CONTENTS----- --- --- --- --- ------ --- --- --- --- ------ --- --- --- --- ----- --- ----XIV

ACKNOWLEDGEMENTS

It's been an amazing journey to explore in a foreign country, to pursue the training satisfying my curiosity, to search for the hope of the patients on a research bench. The past five years in this beautiful campus has shaped me into a better version of me, who now has much more resistance to failures, responsibility to the world, and enthusiasm to science.

I would like to first thank my Ph.D. mentor: Dr. Yibin Wang, who sometimes challenges, often guides and always supports me. You have helped this shaping process greatly with your rigorous training in science and your kind comfort to ease the pain of growth. I learned so much from your generosity in treating others and your wisdom in life which will forever be a treasure of mine to keep.

This project has received lots of advice and suggestions from the first day. I would like to thank all the people who helped to make it so wonderful. My committee members Dr. Thomas Vondriska, Dr. Jau-nian Chen and Dr. Reza Ardehali I also want to thank Dr. Steve Clark, Dr. Tracey Johnson, Dr. Douglas Black, Dr. Tomas Ganz, Dr. Ming Guo and Dr. Grace Xiao for your training and support in my project.

I would like to thank my husband Josh Lee, who met me at my bench in my first year and has carried out a colorful life with me ever since. We have walked together in many kinds of weathers and situation, which has made my world much bigger and

my life more meaningful. You are my best companion, when we travel on the road or stay at home.

I would like to thank my dear friend Shuin (Sue) Park, who has been my classmates, my bridesmaid, JoJo's favorite Auntie, and my roommate in the past five years. For many years in the future, I will miss our nerdy talks with the whiteboard and our girls talk with laughter and tears (and lots of beer!). I cannot imagine a graduate school life without you.

To all the lab members in the Wang lab and MCIP faculty and stuff, your companion and support have made me a true bruin just like the sunshine in Los Angeles. I came to the U.S. alone in 2014 Fall, but now thanks to all the people around, I am now with a loving family, a husband and a dog, a son to expect, and many friends and mentors who always back me up to become who I am. I love you all, and will forever appreciate our time spent together.

BIBLIOGRAPHY

BIOGRAPHICAL SKETCH

NAME: He (Iris) Wang

POSITION TITLE: Graduate Student Researcher

EDUCATION/TRAINING

INSTITUTION AND LOCATION	DEGREE	TIME	FIELD OF STUDY
Xi'an Jiaotong University, Xi'an, China	B.S.	09/2009 - 10/2014	Forensic Medicine
Xi'an Jiaotong University, Xi'an, China	B.A.	09/2009 - 07/2014	Business Management*
University of California, Los Angeles	Ph.D.	07/2014 -	Molecular Physiology

Date of advancement to doctoral candidacy: December 13th, 2016
*This is a double-major degree

A. Positions and Honors

Positions in Research

2011 – 2014	Undergraduate Research Assistant, China National Key laboratory of Forensics
2014 –	Graduate Student Researcher, UCLA

Other Professional Experience

2011 – 2014	Senior Student Counselor of Forensic & Medicine Department, XJTU
2012 – 2014	Residency in Shaanxi Provincial People's Hospital
2013 – 2014	Forensic Assistant in Shaanxi Forensic Science Service Center
2016 – 2017	Vice President, UCLA Chinese-American Students and Scholars Seminar
2017 -	President, UCLA Chinese-American Students and Scholars Seminar
2019 -	Senior Graduate Student Mentor

Honors & Awards

2009	Si-Yuan Scholarship	¥3,000
2010	China National Scholarship	¥8,000
2011	First Prize in China 4th National Language Skills Competition	
	Peng-Kang Scholarship	¥5,000
2012	Outstanding senior students Counselor	
	UCLA-CSST Best Poster Presentation of 2013	
	Si-Yuan Scholarship	¥3,000
2014	Outstanding Graduates in XJTU	
	China Scholarship Council Scholarship	$104,000
	UCLA-GBP Incentive program	$3,000
2015	Jennifer S. Buchwald Graduate Fellowship in Physiology	$15,400
2017	American Heart Association Pre-Doctoral Fellowship	$53,688
	UCLA-GBP Incentive program	$3,000
2018	UCLA Cardiovascular Symposium poster presentation award	$500
	UCLA-GBP Incentive program	$3,000

B. Contributions to Science

Publications

1. Zhihua Wang, Xiao-Jing Zhang, Yan-Xiao Ji, Peng Zhang, Ke-Qiong Deng, Jun Gong, Shuxun Ren, Xinghua Wang, Iris Chen, **He Wang**, …, Hongliang Li & Yibin Wang. The long noncoding RNA Chaer defines an epigenetic checkpoint in cardiac hypertrophy ***Nature Medicine*** 22, 1131–1139 (2016)
2. LncRNA MIAT regulates cardiac pathological hypertrophy via ribosomal biogenesis control. **He Wang**, Zhihua Wang, Yifan Wang, Christopher Rau, Chen Gao, Xinshu Ren, Jonelle White, Steven Clarke, Yibin Wang *(In submission)*
3. Ribosome biogenesis: empower the engine for cardiac hypertrophy. **He Wang**, Yibin Wang *(invited review, in submission).*

(All following publications are translated from Chinese)

4. **He Wang**, Yinan Wang, Jinwei Shi, Zheng Chu (2013, January). Appraisal of the basketworks in NO.M1 tomb of the mausoleum at Feng Qi Yuan in Western Han Dynasty. ***The Universe*** (ISSN1006 - 2335)
5. **He Wang**, Yinan Wang, Jinwei Shi, Zheng Chu (2012, December). Four kinds of DNA extraction methods in old bone DNA testing in performance evaluation. ***Medicine and Jurisprudence*** (ISSN1674-7526)
6. **He Wang**, Yinan Wang, Zheng Chu, Jinwei Shi (2012, October). Clarification of in flora containers in NO.M1 tomb of the Zhang Anshi mausoleum (Western Han Dynasty). ***Journal Of Tianjin Medical University*** (ISSN1006 - 8147)
7. Xuewei Zhang, **He Wang**, Zhuo Mao (2012, October). Study on voicing mechanism of Crist Ibis and Its Foxp2 gene. ***Journal of Tianjin Medical University*** (ISSN1006 - 8147)

Presentations

09/2015 From clinic to bench: what do we get? Seminar for Biomedical Education Program, UCLA

08/2013 Biomarkers in saliva: new landscape for periodontal disease. CSST 2013 life science seminar, California NanoSystems Institute, UCLA

Poster Presentations

08/2013 Periodontal diseases: the most common infectious disease in the world. **He Wang**, Samantha Chiang, Xinmin Yan, David T. Wong, CSST program, California NanoSystems Institute, UCLA

09/2016 Myocardial Infarction Associated Transcript (MIAT): a regulator of ribosomal function linking to pathological cardiac growth in heart diseases. Zhihua Wang, **He Wang**, Christopher Rau, Xinshu Ren, Yibin Wang, Cardiovascular Symposium, UCLA

04/2018 lncRNA Miat contributes to cardiac hypertrophy and regulate ribosome expression. **He Wang**, Zhihua Wang, Christopher Rau, Xinshu Ren, Yibin Wang. Cold spring harbor conference, Suzhou, China

07/2018 lncRNA Miat contributes to cardiac hypertrophy and regulate ribosome expression. **He Wang**, Zhihua Wang, Yifan Wang, Christopher Rau, Chen Gao, Xinshu Ren, Jonelle White, Steven Clarke, Yibin Wang. American Heart Association BCVS, San Antonio, TX

10/2018 Matter of translation: lncRNA Miat in cardiac hypertrophy. **He Wang**, Zhihua Wang, Yifan Wang, Christopher Rau, Chen Gao, Xinshu Ren, Jonelle White, Steven Clarke, Yibin Wang. Cardiovascular Symposium, UCLA

LIST OF FIGURES

Figure 1-1. rDNA locus and rRNA structure.

Figure 1-2. Overview of pre-rRNA processing in mammalian cells.

Figure 2-1. Miat is significantly associated with lung weight in isoproterenol treated mice.

Figure 2-2. Miat expression in mice hearts in C57/BJ, BALB/Cj and FVB/nJ strains.

Figure 2-3. Miat knockdown protects NRVMs from PE induced cellular hypertrophy.

Figure 2-4. Generation of Miat knockout (Miat KO) mouse model.

Figure 2-5. Miat KO mouse is resistant to TAC-induced hypertrophy.

Figure 2-6. Cardiac hypertrophic marker genes expression in TAC mouse model.

Figure 2-7. Cardiac functions are protected in Miat KO TACed hearts.

Figure 2-8. Cardiac functions are protected in minipump mouse model.

Figure 2-9. Hypertrophic marker gene expression in minipump mouse model.

Figure 3-1. Ribosome subunits assembly process.

Figure 3-2. Nucleolin structure and known binding sites.

Figure 4-1. Miat regulates ribosomal gene expression in the heart.

Figure 4-2. Schematic illustration of puromycin labeling assay.

Figure 4-3. Miat is required for elevated protein synthesis.

Figure 4-4. Miat regulates ribosome assembly genes and pre-rRNA.

Figure 4-5. Miat dominantly expresses in the nucleus and does not translocate under stress.

Figure 4-6. Design of Northern blotting probes ITS1 and ITS2.

Figure 4-7. Miat KO abolishes pre-RNA processing.

Figure 4-8. Ribosome profiling reveals less ribosomes are assembled under growth in Miat KO MEFs.

Figure 5-1. Miat contains multiple NCL binding sites.

Figure 5-2. Miat binds to NCL and is required for NCL-pre-rRNA binding.
Figure 5-3. Miat-NCL interaction mediates protein synthesis in cardiomyocytes synergistically.
Figure 5-4 PE induces nucleoli formation in NRVMs.
Figure 5-5. PE induces nucleoli formation in NRVMs is Miat dependent.
Figure 5-6. Miat is required to maintain cell cycle and cell size in MEF.

LIST OF TABLES

Table 1-1. Ribosome biogenesis factors
Table 2-1. List of lncRNA regulators in cardiac development and diseases.

GLOSSARY

Cardiovascular disease (CVD)

Phenylephrine (PE)

Knockout (KO)

Knockdown (KD)

Mitogen-activated protein kinase (MAPK)

Mass spectrometry (MS)

Preinitiation Complex (PIC)

the GTPase-activating protein(GAP)

Cryogenic electron microscopy (cryoEM)

the internal guide sequence (IGS)

ribosomal RNAs (rRNAs)

ribosomal proteins (RPs)

nucleolar organizer regions (NORs)

ribosomal DNA (rDNA)

upstream promoter elements (UPE)

TABLE OF CONTENTS

CHAPTER I. CARDIAC HYPERTROPHY AND TRANSLATION--- --- --- --- --- ---1

1.1 Cardiac hypertrophy

1.1.1Transcriptional regulation of cardiac hypertrophy

1.1.2Translational landscape of cardiac diseases

1.2 Mechanisms regulating muscle mass

1.2.1 Translation efficiency

1.2.1.1 Initiation

1.2.1.2Elongation

1.2.1.3Termination and recycling

1.2.2 Translation capacity

1.2.2.1 The ribosome

1.2.2.2Ribosome biogenesis

1.2.2.3The ribosomal genes

1.2.2.4 rDNA transcription

1.2.2.5Processing and maturation of pre-rRNA

1.2.2.6Key regulators of ribosome biogenesis

1.3 Thesis goal

CHAPTER II. LONG NONCODING RNA MIAT REGULATES CARDIAC HYPERTROPHY UNDER STRESS--- --- --- --- --- ------ --- --- --- --- ------ --- --- --- -- ---13

2.1 Long noncoding RNAs in the heart

2.2 Identification of Miat

2.3 Material and methods

2.3.1 Animals

2.3.2 Cell cultures

2.3.3 Transverse aortic constriction surgery

2.3.4 Echocardiography.

2.3.5 Real-time RT–PCR analysis

2.3.6 RNA deep-sequencing and transcriptome analysis

2.3.7 Immunoblotting analysis

2.3.8 Statistical analysis

2.4 Results and findings

2.5 Discussion

Acknowledgements

CHAPTER III. RIBOSOME BIOGENESIS AND RNA BINDING PROTEIN NUCLEOLIN --- --- --- --- --- ------ --- --- --- --- ------ --- --- --- --- ------ --- --- --- --- ----- ---30

3.1 Introduction

3.2 Nucleolus, the birthplace of ribosomes

3.3 Nucleoli and cardiac diseases

3.4 Nucleolin, a critical nucleolar protein for ribosome biogenesis

3.5 NCL in cardiac diseases

CHAPTER IV MIAT REGULATES RIBOSOMAL GENE EXPRESSION AND PROTEIN SYNTHESIS IN CARDIOMYOCYTES--- ------ ------ ------ ------ ------ ---- ---35

4.1 Introduction

4.2 Methods and materials

4.2.1 Protein synthesis labeling *in vitro* and *in vivo*

4.2.2 Northern blotting

4.2.3 Ribosome profiling

4.3.4 Subcellular RNA extraction

4.3 Results and findings

4.4 Discussion

Acknowledgements

CHAPTER V. MIAT BINDS TO NUCLEOLIN AND REGULATES PROTEIN SYNTHESIS AND NUCLEOLI FORMATION IN CARDIOMYOCYTES--- ------- ---50

5.1 Introduction

5.2 Methods and materials

5.3 Results and findings

5.4 Discussion

Acknowledgements

CHAPTER VI. SUMMARY --- ------ ------ ------ ------ ------ ------ ------ ----- ------- ------ ---60

6.1 Working model

6.2 Future perspectives

REFERENCE--- ------ ------ ------ ------ -------- ------ ------ ----- ------- ------ ------ ------ ------ 62

CHAPTER I. CARDIAC HYPERTROPHY AND TRANSLATION

1.1 Cardiac hypertrophy

Cardiovascular disease (CVD) remains the leading cause of death worldwide. In the United States, CVD was responsible for 840,768 deaths in 2016. The annual total cost of CVD in the United States was a heavy economic burden to the health care system, estimated at $351.2 billion in 2014-2015 (22). Cardiac hypertrophy is a compensatory change of cardiac wall thickening, myocardial weight increase and myocardial remodeling that occurs in the heart under pressure overload. This initial compensatory mechanism may lead to heart failure if the stress sustained. As adult cardiomyocytes are terminal-differentiated, cellular growth of cardiomyocytes is the major reason, which is regulated by gene expression. Previous studies of pathogenesis of cardiac hypertrophy have been focusing on gene transcription, metabolic changes and signal transduction regulations etc. Although enhanced protein synthesis was observed more than 80 years ago and is one of the most consistent changes during the cardiac hypertrophy process across species, little is known about the regulation and underlying mechanisms of protein synthesis and translation in cardiac hypertrophy.

1.1.1 Transcriptional regulation of cardiac hypertrophy

Thanks to many advanced technologies in biomedical science, i.e. microarray, deep RNA sequencing, ChIP-sequencing and mass spectrometry, the gene expression pattern of cardiac hypertrophy have been reveal at multiple layers. Overall, hypertrophy of cardiac myocytes is the result of the imbalance expression between pro-hypertrophic factors and anti-hypertrophic factors. This has been observed at chromatin structure and histone modification level(23, 24), DNA methylation level

(25, 26), transcriptome level including RNA splicing events, non-coding RNAs and microRNAs ((27, 28)), signaling pathways, especially MAPK signaling pathway((29)) and proteomics level(30, 31).

1.1.2 Translational landscape of cardiac diseases

Gene expression in the heart development and diseases has extensively been studied at the transcription layer, largely neglecting translational regulation. As one of the most fundamental activities of a living cell, translation is the process where mRNAs are decoded into polypeptides, which then be processed and folded into functional proteins. It has been noticed back in the 1950s that both translation efficiency and capacity in cardiomyocytes are actively regulated under hormonal stimuli(12, 32). In the cardiac hypertrophy, translation efficiency and capacity are up-regulated and such phenomena persist throughout hypertrophy process as described by Morgan and Nagai via multiple animal studies(6, 7). Mechanistically, mTOR pathway has shown to be critical for regulating translation efficiency by phosphorylation critical translation initiation factors eIF4B and translation capacity through S6Kinase signaling pathway and ribosome assembly factor Maf1 which affect ribosome biogenesis in the cell(11, 33, 34). However, mTOR mediated cellular growth is not specific to the cardiomyocytes, nor it is close to a complete picture of translation regulation in the heart.

Recent years, due to application of Ribo-seq, which captures the footprint of mRNA loading to ribosomes, we could take a closer look at the translatome of human heart. Heesch et al. by examining 80 healthy or dilated human hearts, identified novel

translation events in the heart and extensive translational control of cardiac gene expression in a process-specific manner (31). Widespread translational control in fibrosis was reported, too(35). These findings highlight the importance of translational regulation in the cardiac diseases and raise great interest in the field to uncover underlying mechanisms.

1.2 Mechanisms regulating muscle mass

Adult cardiac tissue is adaptive to pressure overloading and increased physical activity by up-regulating catabolism. The hypertrophy of cardiac tissue is dictated by the balance of protein synthesis and degradation. Sanford's study using a L-thyroxine injection induced rat cardiac hypertrophy model, showed that in hypertrophic hearts, the driven force is enhanced protein synthesis which increased by 22% while the protein degradation rate remains relatively constant, especially in the long term (36). Protein synthesis in a tightly regulated energy-consumptive process. To achieve higher protein synthesis rate, the cell must increase translation efficiency, which is the speed of new polypeptide generated by per existing ribosome, or to increase translation capacity, the number of total ribosomes in the cell.

1.2.1 Translation efficiency

Given an existing ribosome, the translation of mRNA consists of three steps: translation initiation, translation elongation and translation termination and ribosome recycling whereas the initiation is considered as the rate-limiting step.

However, there is increasing evidence showing elongation also regulated the speed of translation and can act in a mRNA specific manner(37, 38).

1.2.1.1 Initiation

In the cytosol, initiation starts with the assembly of Met-tRNAi-eIF2-GTP complex. Free small (40S) subunits of ribosomes, along with eIF1A and eIF3 are recruited to form the 43S Preinitiation Complex (PIC). With the eIF4s (eIF4F, eIF4E, eIF4A and eIF4G), the 5' cap of mRNA is captured by the 43S PIC and prepared for translation as the mRNA secondary structure is unwind by eIF4A. The 43S PIC and eIF4F-mRNA then scan the mRNA sequence for the start codon AUG, which form an anticodon pair of Met-tRNAi to trigger the hydrolysis of the GTP-eIF2 bound, with eIF5 functions as the GTPase-activating protein(GAP). The GDP-eIF2, with assist of eIF5B, then releases other complex to enable recruitment of large (60S) ribosomal subunit. This 80S translation machinery is committed to read codons and insert corresponding aminoacyl-tRNAs and generate the first peptide bind between two amino acids.

Initiation has been studied extensively as the rate-limiting step of translation and it responds to many stress, nutrients and growth factors. Among known mechanisms of initiation regulation, it is not surprising that mTOR is the master regulator, as it senses and processes a wide range of nutrients, growth factors and mechanical stress. eIF4E binding protein-1 (4EB-P1) inhibits initiation while binding eIF4E, once phosphorylated by mTOR, the eIF4E is released and binds to the 5' cap of mRNA.

P70S6K also shows strong effect on protein synthesis, however, the detailed mechanism remains unclear.

1.2.1.2 Elongation

Elongation is the step when amino acids are added to form peptides until the stop codon (UAA, UGA, UAG) is read. It is cyclic and requires charged tRNAs conjugated with amino acids, aminoacyl-tRNA synthetases and elongation factors. During elongation, 1) specific tRNA is sorted from the pool by tRNA synthetases to deliver to the elongation factor for ribosome entry; 2) a peptide bond with the previous amino acid is formed once the tRNA reaches the ribosome; 3) the ribosome trans-locates to read the next codon.

In this step, elongation factor 2 (eEF2) is the well know knot for regulation. When there's a decreased ratio of ATP/AMP in the cell which suggesting a higher demand of other cellular activities other than protein synthesis, AMPK activates eEF2k which phosphorylates and inactivates eEF2 to lower down global translation rate. eEF2k also contains several mTOR phosphorylation residues which shows opposite function compared to AMPK mediated kinase activity. Specifically, p70S6K phosphorylates inhibitory site in eEF2k to permit elongation process.

1.2.1.3 Termination and recycling

Termination occurs when the stop codon reaches the ribosome. Eukaryotic Release Factors 1 (eRF1) recognize the stop codon and eRF3 hydrolyses the GTP to release

the polypeptide. Several components of the translation machinery, including 40S and 60S subunits, tRNA, and mRNA are disassembled by eIF3 and recycled.

Fewer studies focus on translation termination and recycling compared to the first two steps, but there is more evidence stating this last step is essential to the overall translation rate in the cell as it largely determines available free ribosome numbers in the cytoplasm. One example is that in bacteria, defect in IF3 releasing the tRNA from the 30S subunit halts reassembly of the 70S ribosome(39). Sogorin et al. showed that in a cell free system, the termination and initiation is coupled within polyribosomes(40).

1.2.2 Translation capacity

Translation capacity allows sustained increased protein synthesis in the cell. Ribosome biogenesis is a tightly controlled, step-wise process to generate new ribosomes. Although this is a key capacity to promote protein synthesis in a cardiomyocyte under growth stimulation, it has been poorly understood so far.

1.2.2.1 The ribosome

The ribosome has been considered as an honest machine to read mRNAs. This complicated organelle is composed of 4 ribosomal RNAs (rRNAs, 5S, 5.8S, 18S, 28S) and 80 ribosomal proteins (RPs). rRNAs are non-coding ribozymes which forms the backbone of a ribosome for the RPs to assemble. The mature 80S contains 2/3 rRNA and 1/3 protein content, with a small subunit 40S composed of 18S rRNA plus 33 RPs and the large 60S subunit composed of 5S, 5.8S, 28S plus 50 RPs. Recent years, single-

particle cryoEM has revealed the near-atomic structure of the human ribosome(41), which has provided structural basis of specific molecular interactions within the translation machinery and subunit interface, to facilitate ribosome-targeting drug development.

1.2.2.2 Ribosome biogenesis

Ribosome biogenesis is a great effort to the cell: all three RNA polymerases, more than 200 assembly factors and 80 ribosome proteins are required to generate a new ribosome.(42) This process is strictly controlled in time and space, which involves complicated steps of DNA transcription, processing, maturation and assembly of two subunits.

Morgan was the first one answered the question of how much does ribosome biogenesis contribute to protein synthesis in a hypertrophic heart. In the rat cardiac hypertrophy model, he showed it was associated with a 25% greater content of rRNAs, termed capacity for protein synthesis(6).

1.2.2.3 The ribosomal genes

Human genome contains more than 400 copies of a 43kb ribosomal DNA (rDNA). They are tandemly arrayed in the nucleolar organizer regions (NORs) on five pairs of chromosomes (Figure 1-1)(43). The coding region which contains the sequences from 18S to 28S (pre-45S) is 13kb, and the internal guide sequence (IGS) contains key regulatory elements for the transcription of pre-45S. In humans, both the upstream

promoter elements (UPE) and the core promotor region have been identified fundamental for transcription initiation(44).

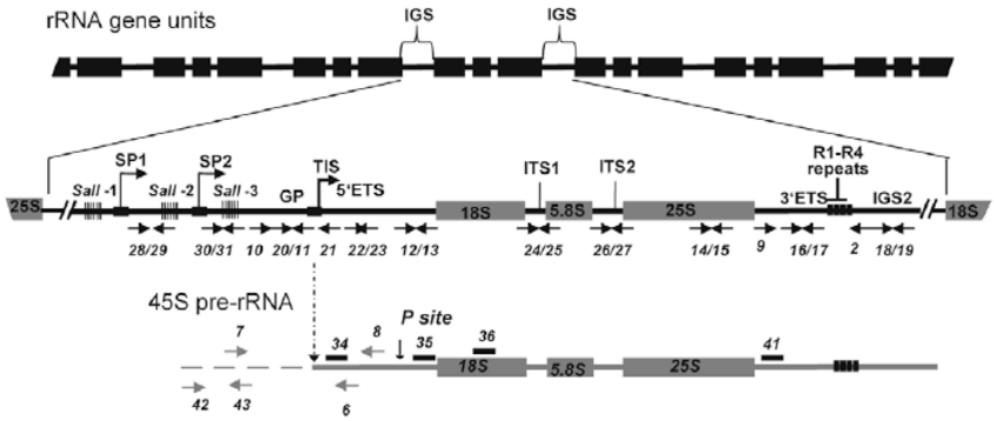

Figure 1-1. rDNA locus and rRNA structure. Modified from Frederic Pontvianne et al (1, 2).

1.2.2.4 rDNA transcription

The *de novo* synthesis of rRNA marks the first rate-limiting event in ribosome biogenesis. The Pol I is dedicated to transcribing 45S pre-rRNA while Pol II to ribosomal protein mRNAs and Pol III to 5S rRNA and tRNAs.

The transcription of Pol I requires the formation of the PIC with the core players upstream binding protein (UBF), the selectivity factor (SL1), transcription initiation factor (TIF-1A) proteins. UBF forms a dimer that binds to UPE and the core promotor region to recruit other initiation proteins including SL1 to the rDNA and is regulated by nutrient and hormonal signals. The SL1 complex brings in necessary transcription factors like TATA-binding protein and their associated factors. TIF-1A is the protein recruits the Pol I complex to start the transcription. UBF and SL1 are kept bounded to the promotor region during elongation, and the transcription is completed when termination elements at the 3'end stalls the movement of Pol I.

1.2.2.5 Processing and maturation of pre-rRNA

Processing and maturation of pre-rRNA is a series of essential steps to cut and fold 45S rRNA into 28S, 18S and 5.8S rRNA for ribosome assembly (Figure 1-2). Simultaneously with the transcription, cleavage sites that mark the internal transcribed spacers(ITS) and external transcribed spacers(ETS) are recognized by enzymes for removal and degradation. Many critical steps including removal of the ITS1 and the adding of ribosomal proteins happens in the membrane-less region inside of nucleolus. These steps require coordination of many assembly factors and

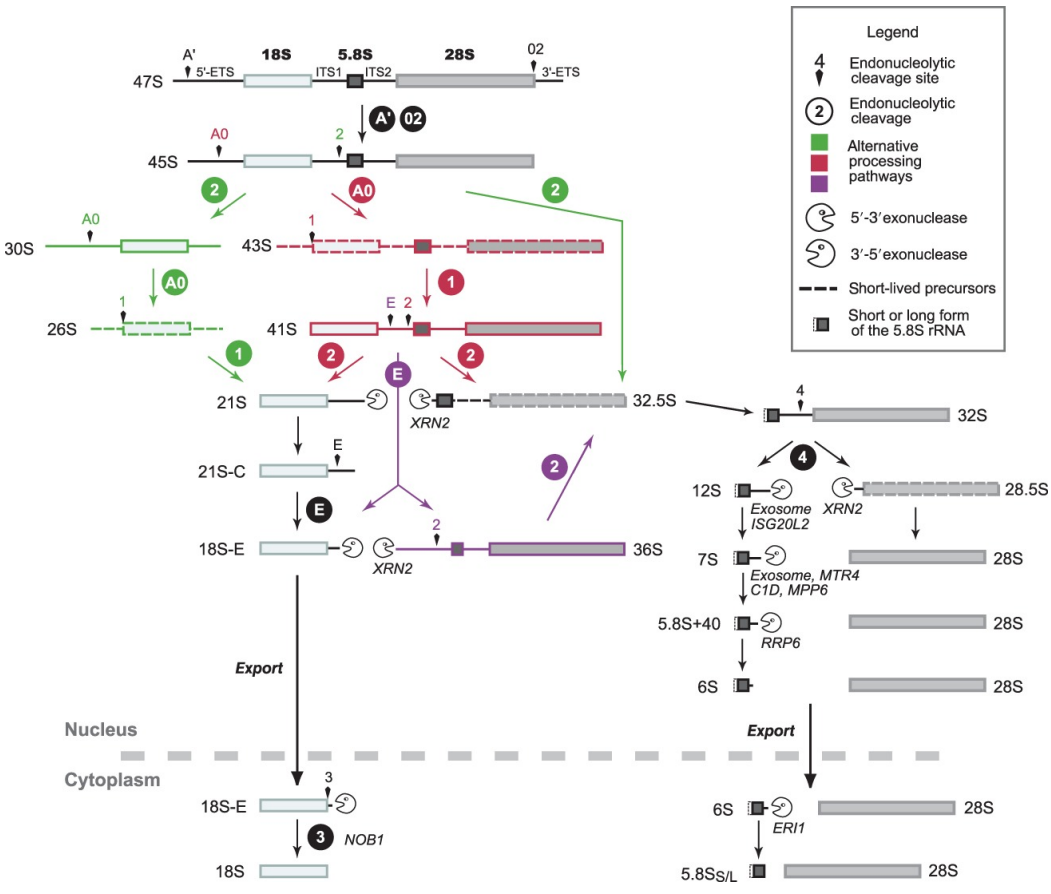

Figure 1-2. Overview of pre-rRNA processing in mammalian cells (human and murine). Cleavage of the 45S (47S) pre- rRNA can start in the 5′-ETS (red) or in the ITS1 (green). Pre-rRNA is processed stepwise by exonucleases to produce 18S, 5.8S and 28S transcripts. Modified from Anthony K. Henras et al. (14)

exporting factors which are not yet well studied in mammalian cells. Finally, pre-40S and pre-60S particles are exported into cytoplasm for protein synthesis.

1.2.2.6 Key regulators of ribosome biogenesis

Current known regulators of ribosome biogenesis are quite limited to signaling pathways. PI3K/Akt/mTOR and ERK pathways phosphorylate the PIC complex (UBF and TIF-1A) to regulate the transcription of rDNAs(45, 46); CDK2/cyclin E kinase phosphorylate TIF-1A and positively regulates rDNA transcription(47); AMPK is shown to stabilize the association between TIF-1A and SL1(48). Figure 1-3 shows key pathways regulates ribosome biogenesis and table 1-1 lists current findings of essential regulatory proteins of ribosome biogenesis process.

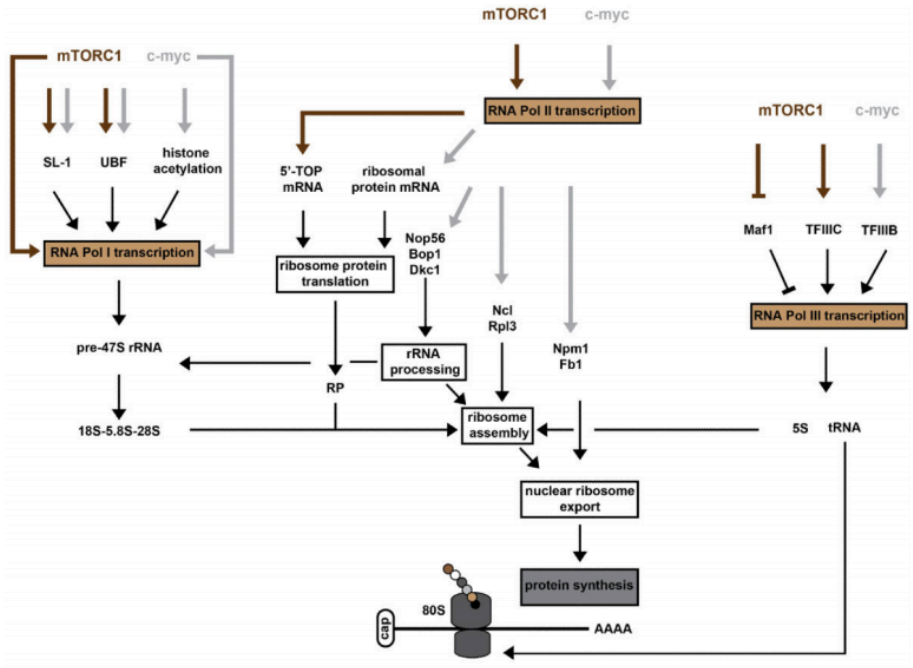

Figure 1-3 Key pathways regulates ribosome biogenesis. mTORC1 regulation is indicated in black while c-myc in gray. Based on RNA Pol I, II or III activity, key responsive proteins are grouped based on stage of ribosome biogenesis. Modified from Katherine I. Farley-Barnes et al(5).

Table 1-1 Ribosome biogenesis factors

Gene name/symbol	Functions	Reference
5'-3' XRN2	Exonuclease acting in 5'-3' direction for first cleavage step of pre-rRNA	(49)
Nop56	Subunit of C/D-box snoRNPs	(50-52)
Nop58	Subunit of C/D-box snoRNPs	(53, 54)
FBL	Nucleolar component, associates with U3, U8, U13 snoRNAs and 2O'methltransferase	(55-58)
NCL	rDNA transcription, pre-rRNA processing, ribosome assembly	(59, 60)
NPM	Nucleolar protein, pre-rRNA processing, RP assembly	(61, 62)
NIP7	3' end cleavage of pre-rRNA	(63, 64)
FTSJ3	Methyltransferase for 34S pre-rRNA processing and 40S subunit assembly	(64)
BOP1	Early rRNA processing	(65, 66)
DDX family	RNA helicases, rRNA folding, microRNA synthesis	(67, 68)

1.3 Thesis goal

To explore the mechanisms of cardiac hypertrophy, we aimed to focus on understanding translational regulation in cardiomyocytes. Currently, there is very little is known about cardiac ribosomes, the regulation of cardiac gene translations, how is translation and proteome regulated in the development and diseases. These

are important areas to explore so to expand our current knowledge of cardiac hypertrophy and broaden potential therapeutic targets.

CHAPTER II. LONG NONCODING RNA MIAT REGULATES CARDIAC HYPERTROPHY UNDER STRESS

2.1 Long noncoding RNAs in the heart

Since the completion of Encyclopedia of DNA Elements (ENCODE) project in 2010, numerous studies highlighted the importance of non-coding transcripts in the human development and diseases. Classified by the size more than 200 nucleotides and poor potential to encode a protein, long non-coding RNAs (lncRNAs) not only show highly cell type specificity, but also are in response to many signaling pathways and under developmental or pathological conditions.

In the heart, lncRNA Fendrr and Braveheart have been identified as crucial players in embryonic development and cardiac lineage commitment(69, 70). Cardiac specific lncRNA Mhrt is downregulated in transverse aortic construction (TAC) induced cardiac hypertrophy model and trigger the isoform switch from Myh6 to Myh7 by directly binding to chromatin-remodeling protein Brg1(71). LncRNA Chast is upregulated in cardiac hypertrophy and induces pro-hypertrophic transcription factor NFAT to promote cardiac remodeling(72). Chaer is another example of how lncRNAs regulate early hypertrophic events precisely in the heart. By transient interaction with EZH2, a polycomb repressive complex 2 (PRC2) subunit, the H3K27 tri-methylation is reduced at the promotor regions of pro-hypertrophic genes, thus, enhanced expression of Anf and Myh7 are turned on soon after stress in the mice. Loss of Chaer at early time point of press-overload animal models shows protective

effect to the heart, at both gene expression and cardiac function levels. Therefore, Chaer-EZH2 defines an epigenetic checkpoint for cardiac hypertrophy(73).

Table 2-1. List of lncRNA regulators in cardiac development and diseases. (modified from Lisa Hobuß et al. *Long Non-coding RNAs: At the Heart of Cardiac Dysfunction?(13)*)

lncRNA	Associated disease	Reported function	Reference
Anril	Coronary artery disease	Biomarker (in diabetic type II patients)	Rahimi et al., 2018
	In-stent restenosis	Biomarker	Wang et al., 2017
	Left ventricular dysfunction	Biomarker	Vausort et al., 2014
Braveheart	Cardiac lineage development	Regulation of chromatin modifications via PRC2	Klattenhoff et al., 2013
Carl	Myocardial infarction	Inhibition of mitochondrial fission and cardiomyocyte apoptosis by sponging miR-539	Wang et al., 2014b
Chaer	Cardiac hypertrophy	Epigenetic modulation of hypertrophic gene expression	Wang et al., 2016
Chast	Cardiac hypertrophy	Induction of hypertrophic cell growth and gene expression	Viereck et al., 2016
Chrf	Cardiac hypertrophy	Sponging of miR-489	Wang et al., 2014a
	Doxorubicin-induced heart failure	Regulation of TGF-β signaling	Chen et al., 2018
Fendrr	Organ development derived from lateral mesoderm	Regulating chromatin modifications via PRC2 and TrxG/MLL	Grote et al., 2013
Ftx	Myocardial infarction	Regulation of cardiomyocyte apoptosis by targeting miR-29b-1-5p	Long et al., 2018
H19	Cardiac hypertrophy	Targeting Ca/calmodulin-dependent protein kinase IIδ (CaMKIIδ)	Liu et al., 2016
	Coronary artery disease	Biomarker	Zhang et al., 2017
	Diabetic cardiomyopathy	Regulation of cardiomyocyte apoptosis by targeting VDAC1	Li et al., 2016b
	Ischemia reperfusion injury	Regulation of necrosis by targeting miR-103/107	Wang et al., 2015
	Myocardial infarction	Activation of autophagy	Zhou et al., 2018
Hotair	Cardiac hypertrophy	Interaction with miR-19	Lai et al., 2017
Lipcar	Cardiac remodeling and heart failure	Biomarker	Kumarswamy et al., 2014
	Coronary artery disease	Biomarker	Zhang et al., 2017
	Left ventricular diastolic function	Biomarker	De Gonzalo-Calvo et al., 2016
Malat1	Atherosclerosis	Regulation of inflammation	Gast et al., 2018
	Cardiac fibrosis after myocardial infarction	Regulation of TGF-β signaling via miR-145	Huang et al., 2018
Mdrl	Ischemia-reperfusion injury	Inhibition of mitochondrial fission and cardiomyocyte apoptosis by sponging miR-361	Wang et al., 2014c
Meg3	Cardiac fibrosis and diastolic dysfunction	Regulation of TGF-β I induced p53 signaling	Piccoli et al., 2017
	Myocardial infarction	Regulation of cardiomyocyte apoptosis	Wu et al., 2018
Mhrt	Cardiac hypertrophy	Regulation of isoform switch Myh6 to Myh7	Han et al., 2014
	Doxorubicin-induced cardiomyopathy	Inhibition of cardiomyocyte apoptosis	Li et al., 2016a
	Heart failure	Biomarker	Xuan et al., 2017
Miat	Cardiac fibrosis after myocardial infarction	Regulation of cardiac fibrosis by interaction with several miRNAs	Qu et al., 2017
	Cardiac hypertrophy	Sponging miR-93	Li et al., 2018
		Sponging miR-150	Zhu et al., 2016
	Left ventricular diastolic function	Biomarker	De Gonzalo-Calvo et al., 2016
	Diabetic cardiomyopathy	Regulation of myocardial hypertrophy and apoptosis	Zhou et al., 2017
	Myocardial infarction	SNP in exon 5 as risk allele for MI	Ishii et al., 2006
Mirt1	Myocardial infarction	Suppression of NF-κB signaling	Li et al., 2017
Nron	Heart failure	Biomarker	Xuan et al., 2017
Sencr	Left ventricular diastolic function	Biomarker	De Gonzalo-Calvo et al., 2016
Wisper	Cardiac fibrosis after myocardial infarction	Alternative splicing of Plod2 mRNA by enabling nuclear localization of TIAR	Micheletti et al., 2017

In addition to cardiac development and cardiac hypertrophy, lncRNAs also involves in myocardial infarction, cardiac fibrosis and has shown great potential as biomarkers and therapeutic targets to advance the diagnosis and treatment of heart diseases(13). Table 1 summarized current findings of lncRNAs in cardiovascular diseases.

2.2 Identification of Miat

lncRNA Miat was first discovered in a GWAS study in Japanese population which compared transcripts differentially expressed in healthy and myocardial infarction patient groups(74). Six SNPs within Miat locus were identified highly associated with MI incidents and were reported to have diagnostic value(75, 76), as indicated by the name *myocardial infarction associated transcript*. In cardiovascular diseases, Miat has shown to be a multi-functional lncRNA in microvascular dysfunction(77, 78), epithelial injury(79), cancer progression(80-82), neurovascular remodeling(83), cardiac fibrosis(84), cardiac hypertrophy(85), coronary atherosclerotic heart disease(86) and cardiac apoptosis(87, 88). Mechanistically, studies in microvascular dysfunctions and fibrosis showed that Miat serves as an endogenous sponge RNA to either compete or interact with micro RNAs (miR-150, miR-214 etc.) to carry out specific functions in the cell. However, the mechanism of how Miat contributes to cardiac hypertrophy and heart failure is largely unknown.

We identified Miat is significantly associated with heart hypertrophy through hybrid mouse diversity panel (89)(HMDP) developed by Dr. Jake Lusis at UCLA. When compared the GWAS and phenotypes of over 100 mice strains received isoproterenol treatment to induce cardiac hypertrophy and heart failure, we found Miat was one of the top hit of mostly associated transcripts(90) with lung weight increase (Figure 1). We confirmed that Miat responses to hypertrophic signal across mice strains by qPCR (Figure 2).

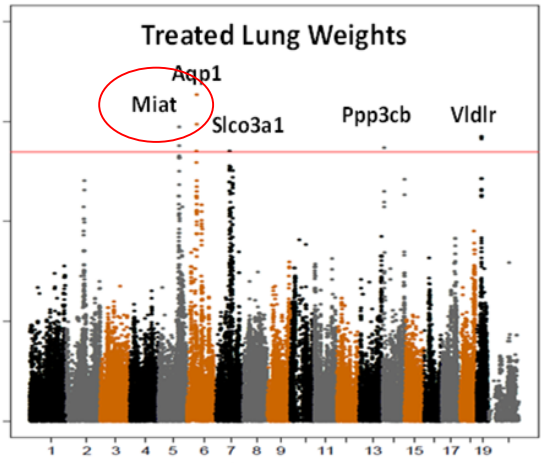

Figure 2-1. Miat is significantly associated with lung weight in isoproterenol treated mice.

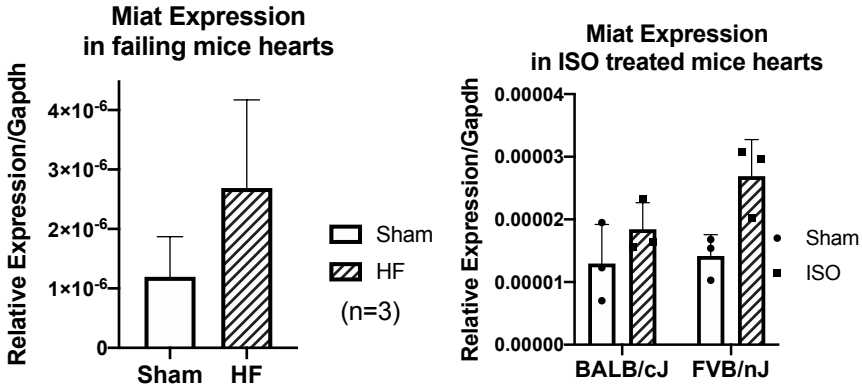

Figure 2-2. Miat expression in mice hearts in C57/BJ, BALB/Cj and FVB/nJ strains.

2.3 Material and methods

This part lists important utilized reagents and methods performed to lead to findings in chapter 2.

2.3.1 Animals

All experimental procedures involving animals in this study were reviewed and approved by the Institutional Animal Care and Use Committees (IACUCs) of University of California at Los Angeles (UCLA) and conformed to the Guide for the Care and Use of Laboratory Animals, published by the US National Institutes of Health. Male or female, 10- to 12-week-old mice in the C57BL/6 background or Miat knockout (Miat KO) were used in this study.

2.3.2 Cell cultures

Neonatal rat ventricular myocytes (NRVMs) were prepared and maintained in Dulbecco's modified Eagle's medium (DMEM) supplemented with 1% insulin–transferrin–selenium (ITS-G, BD Biosciences, CA, USA), 100 U/mL penicillin and 100 µg/mL streptomycin for 24 h before transfection, infection or drug treatment. Immortalized mouse embryonic fibroblasts (MEFs) from C57/BJ or Miat KO background were maintained in DMEM supplemented with 10% FBS, 2 mM L-glutamine, 100 U/mL penicillin and 100 µg/mL streptomycin. Phenylephrine (PE, 50 µM) was used to induce hypertrophy in NRVMs.

2.3.3 Transverse aortic constriction surgery

Transverse aortic constriction (TAC) surgery was performed as described(91) Wild-type and MiatKO male and female mice at 2 months of age were randomly separated into sham and TAC groups; group information was double-blinded between the investigator who performed the surgery and the data analyzer. The mouse was fixed in a supine position with the neck slightly extended. A 20-G catheter was inserted through the larynx into the trachea with care taken not to puncture the trachea or other structures in the pharyngeal region (endotracheal incubation). Ventilation was

performed with a tidal volume of 200 μL, respiratory rate of 120/min, 95% oxygen. Body temperature was maintained as close as possible to 37.0 °C throughout the experiment using a self-regulating heating pad. After disinfection with 2% iodine, the chest cavity was opened by an incision of the left second intercostal space. The aortic arch was dissected from the surrounding tissue. The pericardial sac was opened while a 6-0 suture was passed underneath the transverse aorta and ligated over a 27-G needle, which was removed later to provide a lumen. The chest cavity, muscle and skin were closed layer by layer. Sham-operated mice underwent similar surgical procedures, including isolation of the aorta and looping of the aorta, but without tying of the suture. Mice were observed until recovery in a 37.0 °C heated cage.

2.3.4 Echocardiography.

Transthoracic ultrasonography was performed with a Vevo 2100 system (Fujifilm VisualSonics, Ontario, Canada). Echocardiography was performed before and 4 d after TAC surgery. The inhalational flow of isoflurane was adjusted to anaesthetize the mice while maintaining their heart rate at 450–550 beats/min. The peak aortic blood velocity across the aortic constriction was measured in the pulsed-wave color Doppler mode. Left ventricular function was assessed by M-mode scanning of the left ventricular chamber, standardized by two-dimensional, short-axis views of the left ventricle at the mid papillary muscle level. Left ventricular chamber size and wall thickness were measured for at least three beats from each projection and averaged. Left ventricular internal dimensions at diastole and systole (LVID;d and LVID;s, respectively) were measured.

2.3.5 Real-time RT–PCR analysis

Total RNA was extracted from heart tissue or cells using the TRIzol reagent (Life Technologies, NY, USA). 1 μg RNA was reverse-transcribed into first-strand cDNA using the Superscript III first-strand synthesis kit (Life Technologies, NY, USA) with random primers. Real-time PCR was performed using the CFX96 Real-Time PCR Detection System (Bio-Rad, CA, USA) using the iQ SYBR Green Supermix (Bio-Rad). Values were normalized to Gapdh to calculate relative expression levels. For fractionation, mouse heart was homogenized in Fraction buffer A containing 10 mM Tris-HCl (pH 7.5), 250 mM sucrose, 0.5 mM EDTA and 0.5 mM EGTA. Cell debris was cleared by centrifugation at 200g at 4 °C for 3 min. Nuclei were pelleted at 2,000g at 4 °C for 5 min. RNA from the nuclear and cytosolic fractions were extracted with TRIzol and TRIzol LS reagents (Life Technologies, NY, USA) respectively, and subjected to reverse-transcription followed by real-time PCR analysis, as described above. Data are shown as a percentage of the sum between the value in the nuclei and the value in the cytoplasm, and RNA levels were compared to the levels of the nuclear marker U6 and the cytosolic markers 18S or Actb.

2.3.6 RNA deep-sequencing and transcriptome analysis

RNA deep-sequencing was performed as described previously(91). Total RNA was extracted from WT or Miat KO mice hearts using TRIzol reagents, and it was then reverse-transcribed using the TruSeq RNA Library Prep Kit (Illumina, CA, USA). The libraries were subjected to quality validation using the Agilent Bioanalyzer 2100, and then paired-end sequenced using HiSeq 2500 (Illumina). The resulting reads were mapped to the rn5 database using TopHat2 and visualized on the UCSC browser (http://genome.ucsc.edu). Gene Ontology (GO) analysis was performed with DAVID

Bioinformatics Resources 6.7. Genes with an expression change >1.5-fold were clustered and shown in a heat map (log2 scale) using NetWalker.

2.3.7 Immunoblotting analysis

Cells were washed twice with ice-cold PBS and harvested in protein lysis buffer (50 mM HEPES (pH 7.4), 150 mM NaCl, 1% Triton X-100, 1 mM EDTA, 1 mM EGTA, 1 mM glycerophosphate, 2.5 mM sodium pyrophosphate, 1 mM Na3VO4, 20 mM NaF, 1 mM phenylmethylsulfonyl fluoride, 1 mM DTT and 1× complete protease inhibitor tablet (Roche)). Total cell lysates were separated on 4–12% Bis-Tris gels (Life Technologies) and transferred onto PVDF membranes (Merck Millipore). The membranes were probed with antibodies indicated in the blot. Protein signals were detected using horseradish peroxidase (HRP)-conjugated secondary antibodies and enhanced chemiluminescence (ECL) western blotting detection regents (Thermo Fisher Scientific, MA, USA).

2.3.8 Statistical analysis

Comparisons in multiple groups were analyzed with one-way ANOVA, followed by Student's t-test to calculate the P value between two groups. The sample size was determined by holding the probability of a type I error at $\alpha = 0.05$. Correlation analysis was done by Pearson's r test. Data are presented as mean ± SEM or SD for triplicates.

2.4 Results and findings

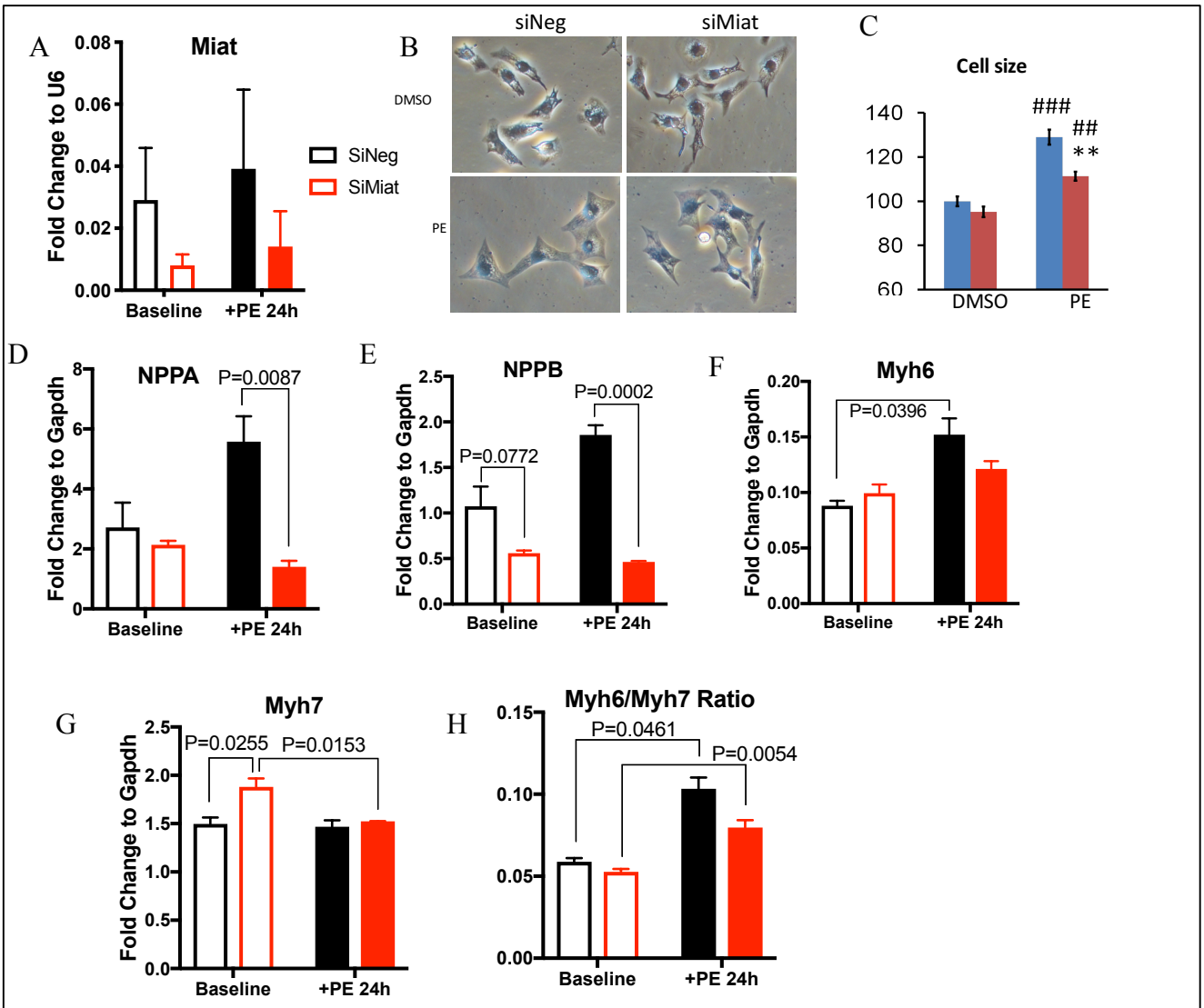

Figure 2-3. Miat knockdown protects NRVMs from PE induced cellular hypertrophy. (A)Confirmation of knowdown efficiency. (B)Representative images of NRVMs received SiNeg, SiMiat transfection and with DMSO or PE(50uM, 24hrs treatment). (C)Quantification of panel (B).(D)(E)(F)(G) q-PCR results of hypertrophic marker gene expression between groups.(H)Myh6 to Myh7 ratio calculated based on expression level in (F) and (G). Statistics: t-test, P values are indicated in each panel.

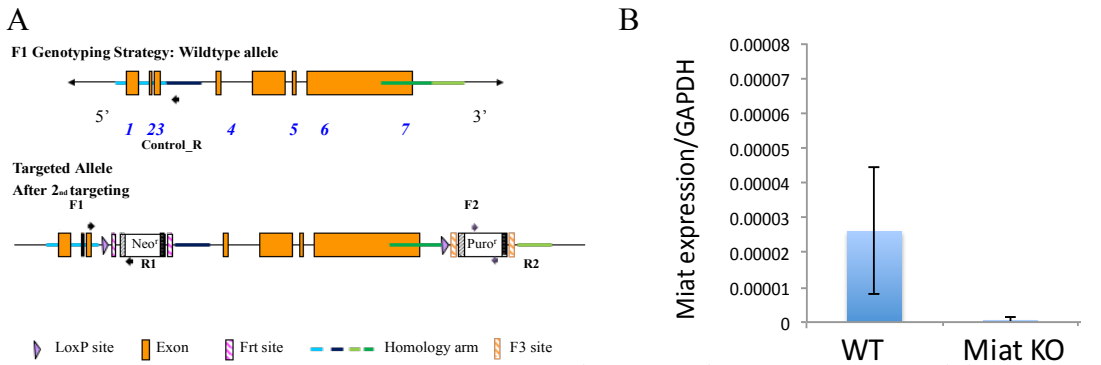

Figure 2-4. Generation of Miat knockout (Miat KO) mouse model. (A)Schematic design of Miat KO using loxP system. (B) Verification of Miat KO in the heart tissue.

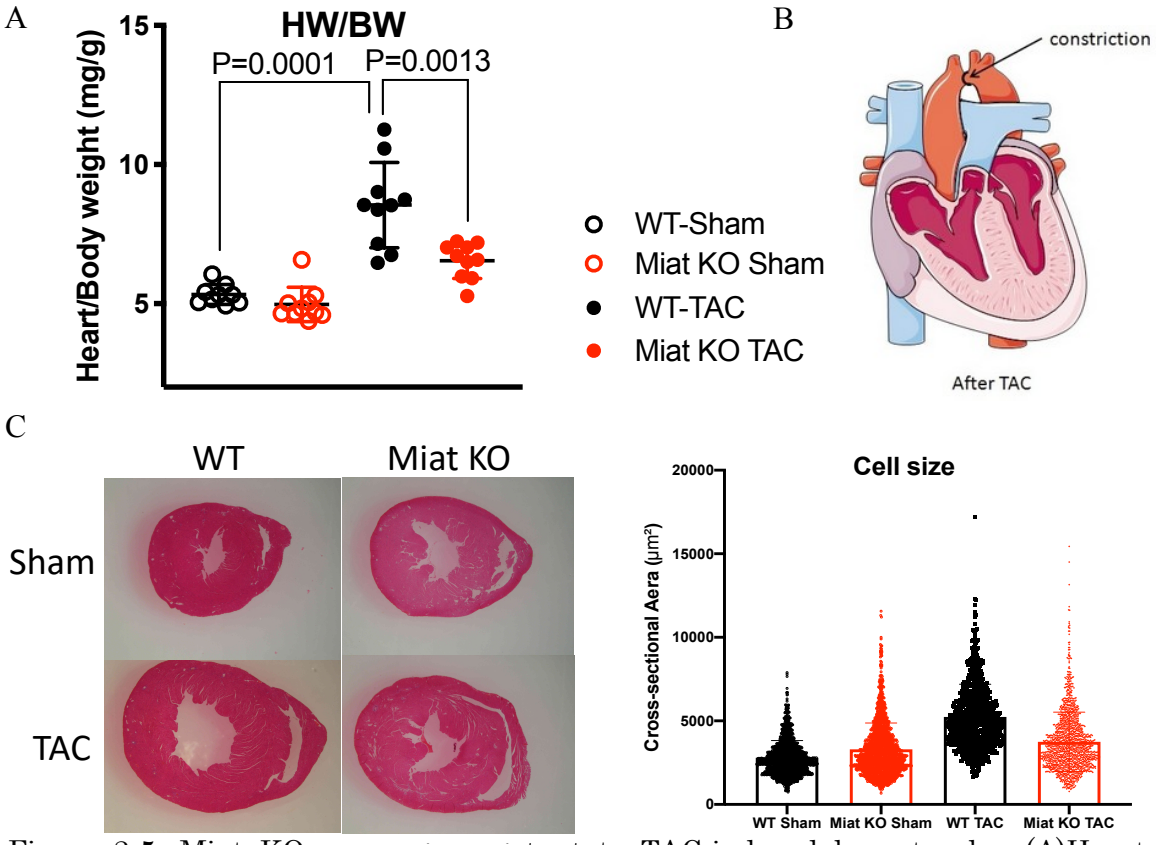

Figure 2-5. Miat KO mouse is resistant to TAC-induced hypertrophy. (A)Heart weight/body weight ratio is measured based on tissue weight when sacrificing the animals in wild-type and Miat KO mice received TAC or Sham treatment. (B)Illustration of TAC surgery. (C) Representative images of cross sections of animal hearts. (D) Cardiomyocyte cell size are measured from WGA staining.

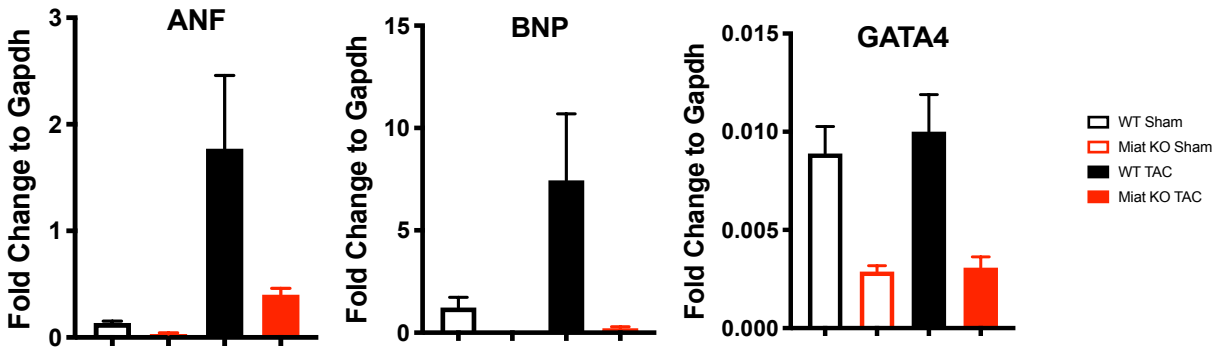

Figure 2-6. Cardiac hypertrophic marker genes expression in TAC mouse model. (A)(B)(C) expression level of ANF, BNP and GATA4 detected by q-PCR from mice left ventricular samples.

Figure 2-7. Cardiac functions are protected in Miat KO TACed hearts. (A)GO analysis of most differentially expressed genes between WT-TACed and Miat KO TACed hearts.(B)Miat expression in four experimental groups.(C)Ejection fraction of animals. Each dot represents an animal. (D)(E) Left ventricular posterior wall thickness in diastolic and systolic conditions.

Figure 2-8. Cardiac functions are protected in minipump mouse model. (A)Illustration of minipump animal model. (B)Miat expression in four experimental groups. (C)Heart weight/body weight ratio of all four groups. Each dot represents an animal. (D)Left ventricular weight verses body weight ratio of all four groups. Each dot represents an animal. (E)Ejection fraction of animals. Each dot represents an animal. (F) Left ventricular posterior wall thickness in diastolic state.

A

Go terms in phenotypes	P-value
Cardiac hypertrophy	6.99e-08
Cardiac fibrosis	9.02e-07
Decreased body weight	4.52e-06
Abnormal pulmonary alveolus morphology	3.69e-05
Enlarged heart	4.15e-05
Decreased ventricle muscle contractility	4.91e-05
Partial postnatal lethality	5.29e-05
Thick ventricular wall	9.04e-05
Increased heart weight	9.21e-05
Embryonic growth arrest	1.07e-04
Abnormal heart morphology	1.29e-04

B

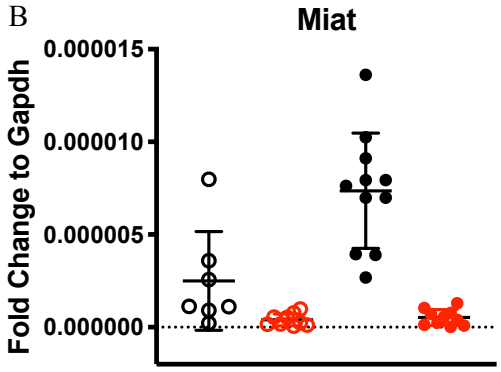

C

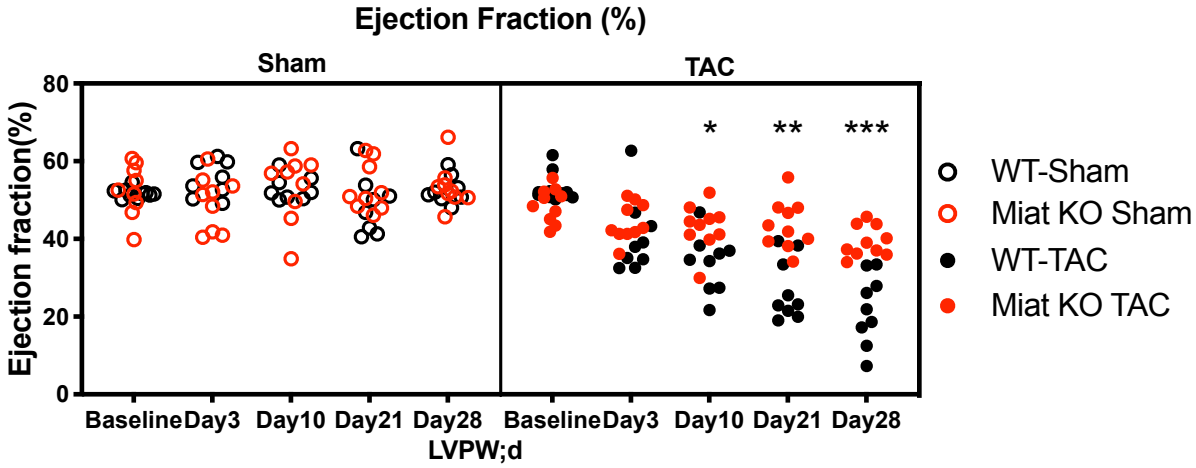

D

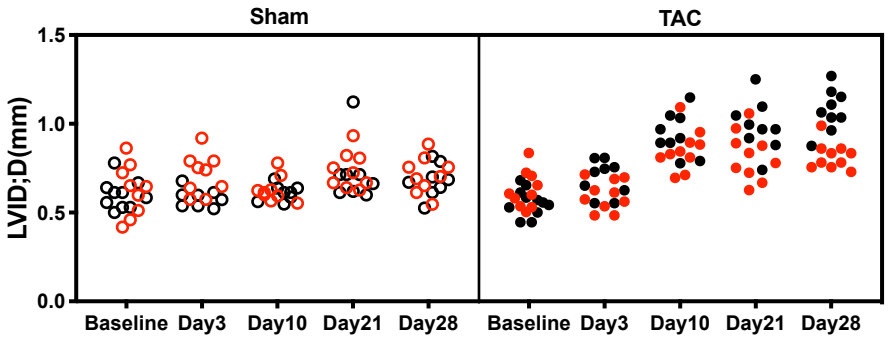

E

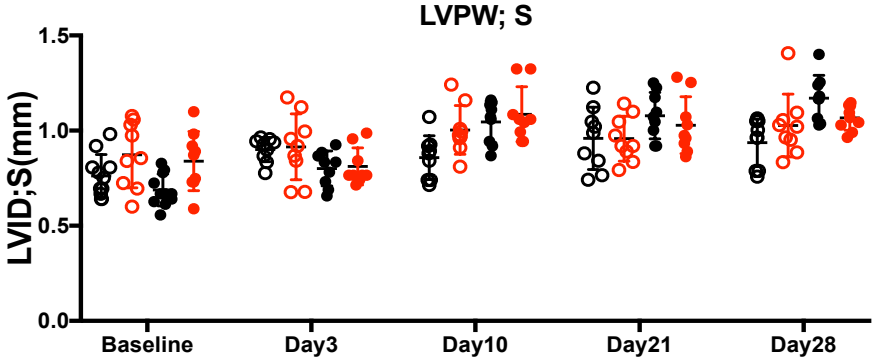

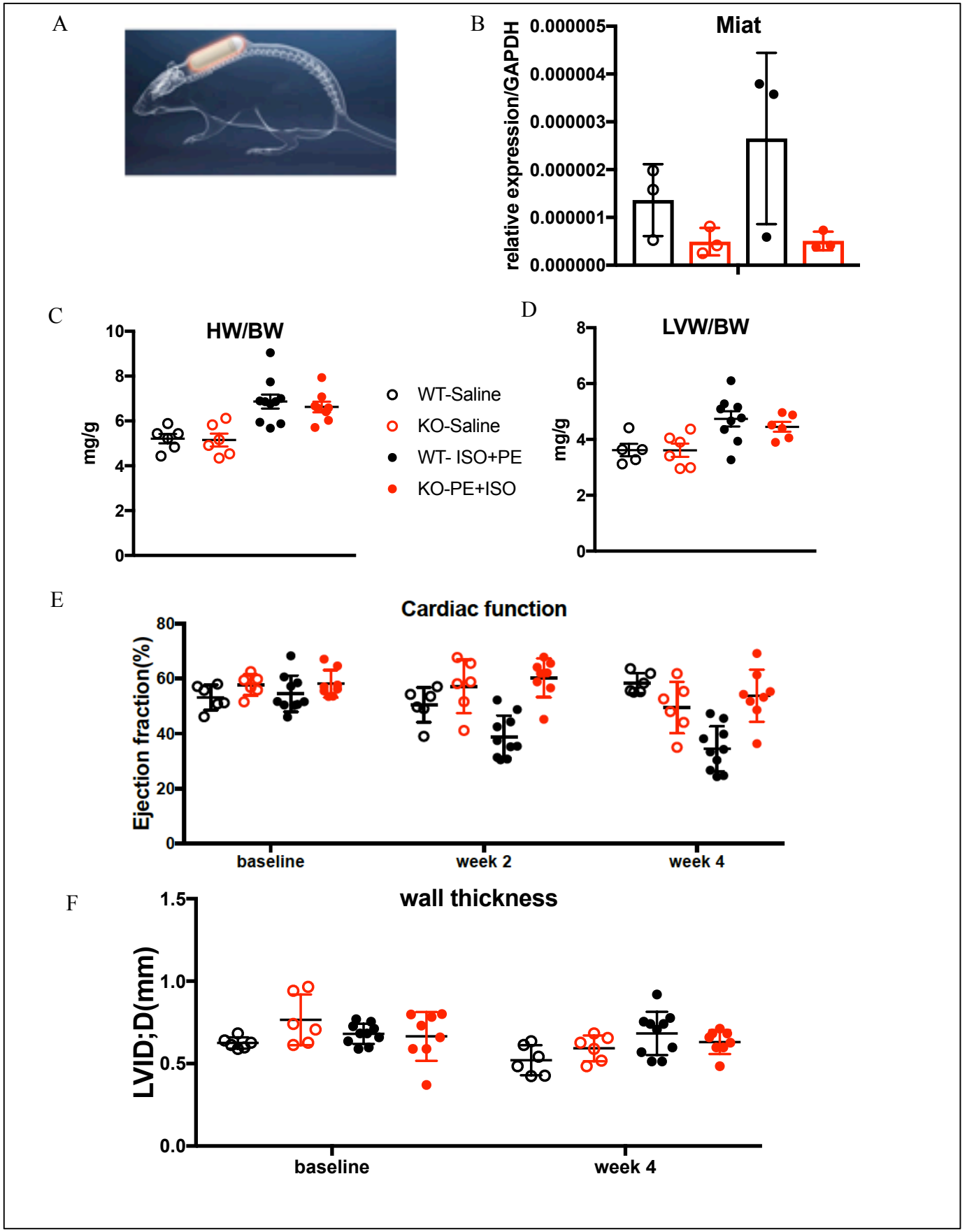
A
B
Miat
relative expression/GAPDH
0.000005
0.000004
0.000003
0.000002
0.000001
0.000000
C
HW/BW
mg/g
10
8
6
4
2
0
WT-Saline
KO-Saline
WT- ISO+PE
KO-PE+ISO
D
LVW/BW
mg/g
8
6
4
2
0
E
Cardiac function
Ejection fraction(%)
80
60
40
20
0
baseline
week 2
week 4
F
wall thickness
LVID;D(mm)
1.5
1.0
0.5
0.0
baseline
week 4

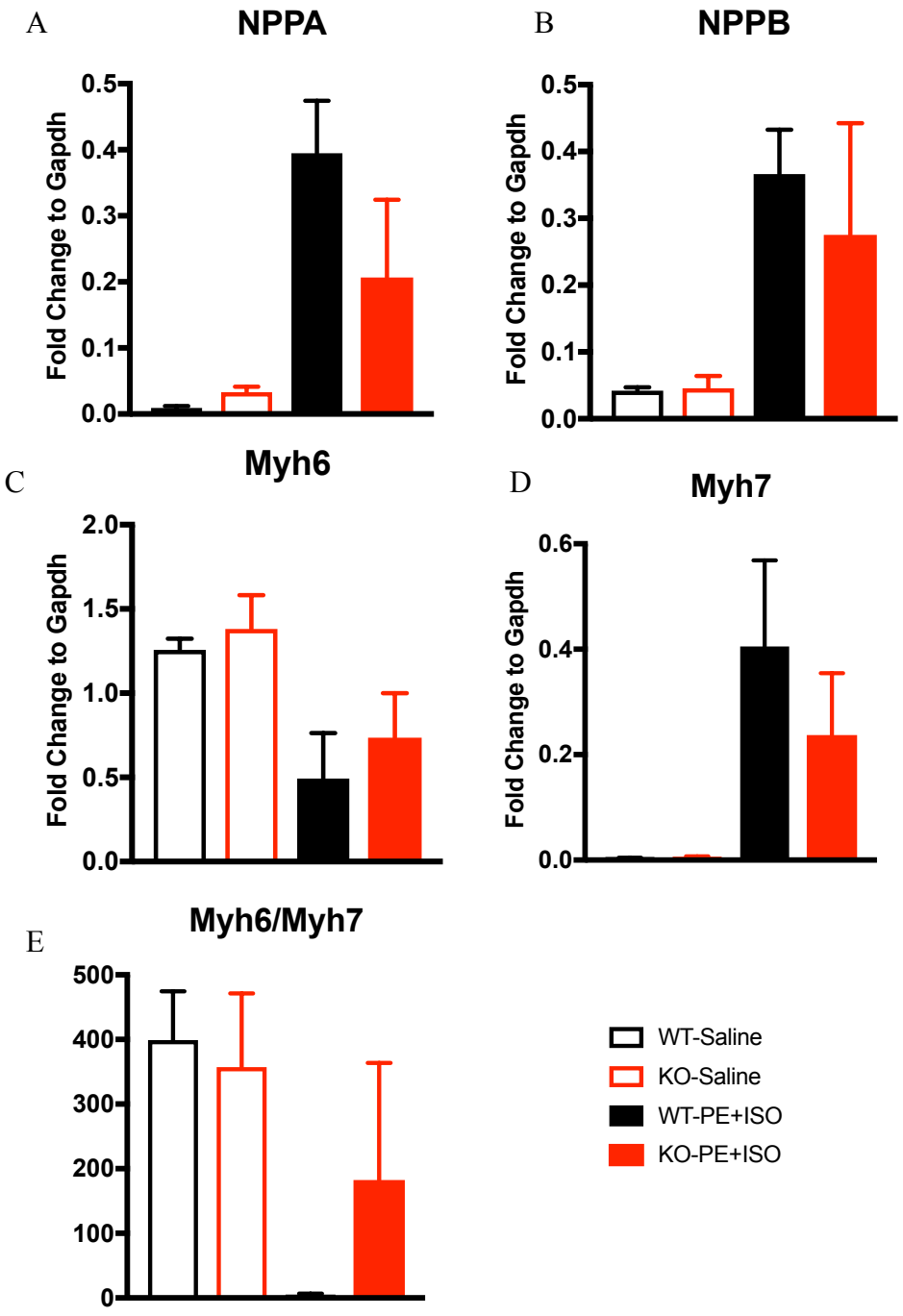

Figure 2-9. Hypertrophic marker gene expression in minipump mouse model.

Miat is necessary for hypertrophy in NRVM

Using NRVMs as an *in vitro* model, we showed that Miat is necessary for hypertrophy induced by PE treatment in NRVMs. When Miat is knockdown by specific siRNA (siMiat) (Figure 2-3A), upon PE treatment, cell sizes are smaller compared to cells transfected with siNeg control (Figure 2-3B&C). We use RT-PCR to detect hypertrophic gene expression after extracting RNAs from whole cell lysate, and NPPA, NPPB (Figure 2-3D&E) expression levels are down-regulated in Miat KD cells, we also observed switched expression of Myh7 and Myh6 in PE treated siNeg cells but not siMiat cells (Figure 2-3 F, G, H).

These data suggest in the NRVM model, loss of Miat expression by siRNA transfection protect NRVMs from hypertrophy mediated by PE treatment. Not only cell sizes are smaller, but all the hypertrophic marker genes detected are lower expressed compared to NRVMs treated with siNeg and PE for 24 hours.

Miat KO protects hearts from stress in both TAC and drug induced mouse hypertrophy models

We firstly generate a knockout mouse model to study the function of Miat *in vivo* (Figure 2-4A) and verified the knockout efficiency in left ventricular (Figure 2-4B). To study how does Miat contribute to cardiac hypertrophy, we used two ways to induce hypertrophy in the mouse, one is pressure-overload model by transverse aortic constriction (Figure 2-5, 2-6, 2-7), the other is a drug induced hypertrophy model by ISO and PE administration delivered by minimum under skin for one month (Figure 2-8, 2-9). In both models, we showed that heart weight to body weight ratio increases in wild type animals after TAC (Figure 2-5A) or ISO+PE delivery (Figure 2-8A),

however, in the Miat KO animals, there is significant decrease of heart weight to body weight ratio compared to wildtype animals after TAC or drug delivery. In the TAC model, we also measured cells size of cardiomyocytes from WGA staining (Figure 2-5 D) where wildtype TACed hearts have larger cardiomyocyte size compared to Miat KO TACed animals. The heart weight and cell size changes are consistent with left ventricular wall thickness we measured by echocardiography (Figure2-7D&E, 2-8F). GO analysis of RNA seq data from left ventricular samples of TAC experiment also confirms our observation as cardiac hypertrophy, thick ventricular wall and enlarged heart are the most affected phenotypes in Miat KO animals (Figure 2-7A). Cardiac function indicated by ejection fraction drops in wildtype mice received TAC (Figure 2-7C) or ISO+PE (Figure 2-8E) treatment while in Miat KO animals, the ejection fraction remains above 40% which suggest that loss of Miat is protective to cardiac function in both hypertrophy models. We also showed that Miat expression response to both types of stress (Figure 2-7B, Figure 2-8B). In Figure 2-6 and 2-9, we detected a panel of hypertrophic marker genes which are highly up-regulated in TACed wildtype mouse hearts and ISO+PE treated wildtype hearts, however, in the Miat KO animals, we observed comparable expression levels of these marker genes at baseline, but much lower after the stress compared to wildtype hearts.

2.5 Discussion

In Chapter 2, we discovered the function of Miat in multiple hypertrophy models. We utilized both in vitro and in vivo models to test how does loss of Miat regulates cardiac hypertrophy progress and our data firstly shows that Miat expression is upregulated

upon PE, TAC and pump stressors. Then, Miat is necessary for hypertrophy in NRVMs and in mouse hearts. As discussed in the introduction, lncRNAs have been considered important regulators of cardiovascular diseases including hypertrophy and Miat adds another example of how loss of a lncRNA leads to strong protective effect of the heart from multiple stress we tested. In summary, we showed that Miat is an essential contributor to cardiac hypertrophy.

We did not test Miat expression or function in physiological hypertrophy models in our study which is a limitation. We will explore the mechanisms of Miat regulating cardiac hypertrophy in the next chapter.

Acknowledgements

Animal breeding and surgery were supported by Dr. Shuxun Ren, Haiying Pu, Yifan (Frank) Wang.

CHAPTER III. RIBOSOME BIOGENESIS AND RNA BINDING PROTEIN NUCLEOLIN

3.1 Introduction

In this Chapter, we firstly review current knowledge of ribosome biogenesis in more depth and details, focusing on nucleolus region and rRNA processing and maturation in eukaryotic cells.

Ribosome biogenesis is a massive effort for the cell to increase the translation capacity by providing more ribosomes. All three RNA polymerases, a large portion of current existing ribosomes, more than 150 non-RPs processing factors, over 70 small nucleolar RNAs (snoRNAs), RNA-helicases, exo & endo-ribonucleases devote together to this coordinated process(92).

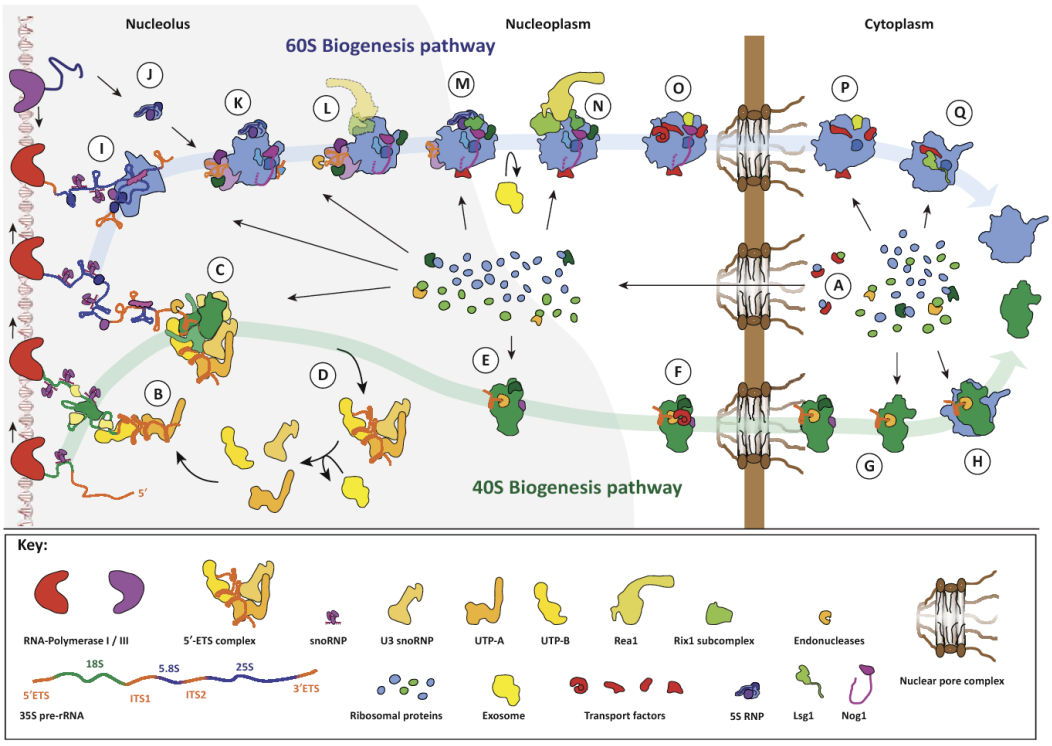

Figure 3-1. Ribosome subunits assembly process. (A)ribosome proteins are transported to nucleus from cytoplasm for assembly. (B–H) assembly of 40S subunit (I–Q) assembly of 60S. Modified from Kressler et al.(3)

3.2 Nucleolus, the birthplace of ribosomes

Ribosome biogenesis starts at the nucleolar, which is a tri-partite membrane-less region in the cell containing a fibrillar center (FC), a dense fibrillar component (DFC) and a granular component (GC). From insides out, the FC is where rDNA is transcripted, then in the DFC, precursor rRNA (45S or 47S) is processed and modified in the GC, it's transported for further assembly into two subunits for ribosome in the nucleus(19, 93). Ribosome biogenesis factors locate in different regions according to their function: early processing factors (UBF, NOP56, NOP58, NCL) stay in the DFC while NPM1 and other assembly factors of a subunit usually are found in the GC(94, 95).

Proteome studies advanced our understanding of nucleoli greatly in recent years as the technology develops. The number of identified nucleolar proteins has increased to over 4,500 from less than 100 10 years ago. Nucleoli proteome is highly conserved with about 90% of yeast nucleoli proteins can find a human homologue. Bioinformatics study of human nucleolar proteome revealed that around 30% of nucleolar proteins are involved in ribosome biogenesis. This is consistent with its function that majority of transcription of rDNA and rRNA processing and subunit assembly are accomplished in this region. Nucleoli also has been identified involving in other cellular activities including mRNA processing, cell cycle control, DNA replication and DNA repair response. It is also important for export of some subsets of mRNAs and tRNA, telomerase production and assembly of some other ribonucleoparticles (RNPs). In the most recent proteome analysis(96-98), more than 250 novel nucleolar proteins were characterized for the first time and many of the functions remain to be explored. There are not a shared motif or structural basis have been discovered in these nucleolar proteins so far, suggesting they likely act in various mechanisms.

3.3 Nucleoli and cardiac diseases

In the heart, nucleolar stress is an early response to myocardial damage(99). It is considered as a stress sensor. By remodeling its morphological and molecular architecture, nucleolar undergoes enlargement or disorganization in response to stress. In ischemic and dilated cardiomyopathy human patients, nucleoli show more fibrillary and less granular, which is an indication of increased ribosome biogenesis

activity(100). When the cell suffers from DNA damage, hypoxia or inhibitors of transcription and ribosomal assembly, the nucleoli segregate and fragment and dismiss(101, 102). Overall, the enlargement and increase of number of nucleoli usually are observed when cells are induced to grow while the shrink of nucleoli indicates the cell is under stress and prepares itself to survival or apoptosis. Portoles et al reported nucleolar organization and protein expression differ in failing human heart but the mechanisms are unknown(100).

3.4 Nucleolin, a critical nucleolar protein for ribosome biogenesis

Nucleolin(NCL) was previously known as C23, it is one of the nucleolar proteins which is an abundant RNA-binding protein. It contains multiple RNA binding regions(RRMs), DNA binding regions and has been shown essential for rDNA transcription and Pol I activity(60). NCL is one of the earliest processor proteins of pre-rRNAs and its proper function is required for cell growth and normal cell size(59, 103, 104).

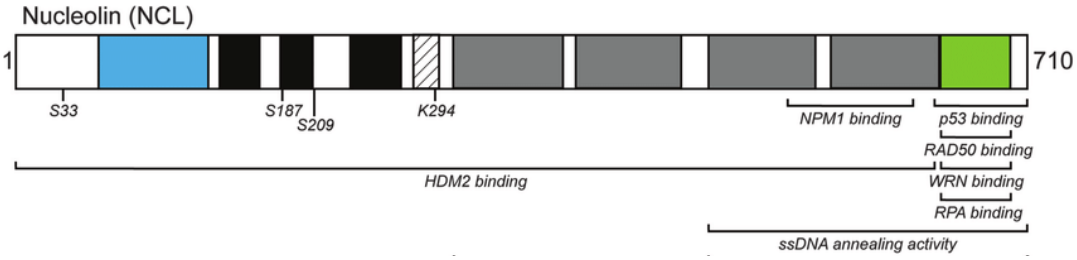

Figure 3-2. Human nucleolin structure and known binding sites. NCL contains a C-terminal domain, four RRMs (in grey) and a N-terminal domain that has multiple functions. (Modified from Daniel Dehany Scott el al (4).

Specifically, NCL binds to rDNA promotor and coding region and is necessary for rDNA transcription as discovered by ChiP-Seq(60). NCL has similar binding patterns to UBTF and the N terminal of NCL interact with Pol I transcription machinery. Four RRMs of NCL specifically bind to nascent rRNA and are involved in the early processing and cleavage steps of rRNA maturation. NCL also recruites ribosome biogenesis factors, especially the U3 snoRNA complex to mediate early rRNA processing. The N-terminal domain interacts with histone protein H1 to modulate chromatin structure and proper folding or rRNA(59).

3.5 NCL in cardiac diseases

Several studies focus on investigating NCL function in muscle and cardiomyopathies. In C2C12 skeletal myoblasts, down-regulation of NCL resulted in loss of proliferation and more apoptosis, suggesting it is primarily associated with cellular growth and survival response of the cell(105). A cardiac specific over-expression of NCL mouse model show more resistance to ischemia-reperfusion injury with reduced infarction size(106). In human patients received heart transplant, there are a nine-fold higher levels of NCL antibodies, indicating that NCL inhibition is associated with allograft failure in heart transplant because endothelial cell proliferation is decreased while apoptosis is increased(107). Although he dominant function of NCL has been recognized in contributing to ribosome biogenesis within the nucleolar, NCL is reported to translocate to nucleoplasm, cytoplasm and cell surface in some cell types(108) and is necessary for virial infection to mammalian cells(109).

CHAPTER IV MIAT REGULATES RIBOSOMAL GENE EXPRESSION AND PROTEIN SYNTHESIS IN CARDIOMYOCYTES

4.1 Introduction

Following discoveries in Chapter II, we found Miat is associated with many differentially expressed ribosomal genes from RNA-Seq analysis, which led us to explore its function in protein synthesis and translation in the heart. In this chapter, we show data of how Miat is required for elevated protein synthesis induced by multiples stressors, how Miat affects ribosome biogenesis in different models. We also detect which could be functional parts of Miat function.

4.2 Methods and materials

4.2.1 Protein synthesis labeling *in vitro* and *in vivo*

We use puromycin to label newly synthesized polypeptides as described (110). In NRVMs, before harvesting, incubate cells with 1ug/ml puromycin for 20min, wash out puromycin by changing back to normal culture medium twice, 10min each. In mouse, i.p. inject puromycin (solved in sterile saline) to achieve a final concentration of 0.4uM/g of body weight. Harvest tissues after 1hour. Puromycin level is detected by western blot as previously introduced.

4.2.2 Northern blotting

Harvest RNA with TriZOL (Invitrogen) per the manufacturer's protocol. Make an aliquot(s) of 3-4 ug of RNA and re-precipitate with 1/10th the volume of 3 M NaOAc, 2-3 volumes of 100% ethanol (cold), and 2 uL pellet paint. Incubate for at least 20 min at -20C, then spin at 4^{o} C for 25 min at 14000 rpm. Wash pellets 2x with 1 mL 75%

ethanol. Spin at 4° C for 5 min at 14000 rpm. Mix and pour 1% agarose gel with formaldehyde. Pour gel and lightly cover with saran wrap to minimize formaldehyde evaporation. Let sit for ~1 hr. Add running buffer (17 mL of 50X Tri/Tri buffer bring to 850 mL with ddH_2O) right before samples are added, again to minimize loss of formaldehyde from gel. Remove the ethanol wash in its entirety from RNA pellets, and then dry the pellets (~10 min). Resuspend RNA pellets in 7.5 uL of formamide in a bench-top shaker for ~5 min. When completely resuspended, add 7.5 uL of loading buffer (14 volumes of loading dye to 1 volume of 37% formaldehyde). Flick to mix and do a quick spin to bring sample to the bottom of the tube. Incubate at 65C for 10 min to denature the RNA. Do *not* spin after this. Load samples (all 15 uL). Run the gel at 140V for 5 min, and then at 110V for 2-3 hours (until the yellow dye in TriTrack buffer is at the bottom of the gel). Once the gel is done running, take it out of the gel box carefully and put into a container to rinse 3x with ddH_2O. Incubate the gel in 0.05 M NaOH for 15 min, shaking gently, to hydrolyze the large pre-rRNA intermediates, which allows for more effective transfer of the large RNAs to the nylon membrane. Be careful to not incubate for any longer than 15 min. Dump the NaOH off the gel, and rinse 3 times with ddH_2O making sure to also rinse the sides of the container. Incubate the gel with ~200 mL of 10X SSC for 5 min, shaking gently, with the nylon membrane (Hybond XL). Set up apparatus for capillary transfer of RNA to membrane. Cross two pieces of saran wrap underneath the apparatus to wrap up the transfer set-up afterwards. Soak wick in 10X SSC. Transfer overnight. Crosslink the membrane, place it in a staining container and pour some 0.025% (w/v) methylene blue staining solution on top of the membrane. Image the membrane for 18S and 28S

bands. Allow to pre hyb for 3 hours at 37ºC. Add 15 to 30 uL of radioactive probe(s) to 500 uL of the prehyb solution that was kept in a locking tube. Denature by heating at 95ºC for 3 min. Remove hyb tube from hyb oven. Remove cap. Add the denatured probe solution to the tube. Wet the cap again with the left over pre hyb solution. Put the cap on the tube. Allow to hybridize overnight at 42º C. Remove hyb solution by dumping into the waste bottle. Wash three time at 42º C for 20 min each wash. Image the membrane.

4.2.3 Ribosome profiling

Protocol modified from Anthony M. Esposito (111).

Make 5%-50% sucrose gradients containing 50mM NH4Cl, 50mM Tris-Acetate pH 7.0 and 12mM MgCl2, DTT 1mM and store at 4°C overnight for linearization. Culture 3*107 cells for each group. Add cycloheximide to the culture to a final concentration of 100 µg/ml and incubate for 30min before harvest. Lysis the cells in lysis buffer (20 Mm HEPES-KOH, pH 7.4, 15 mM MgCl2, 200 mM KCl, 1% Triton X-100 (v/v), 100 µg/mL cycloheximide, 2 mM DTT, and 1 mg/mL heparin) on ice. Centrifuge the lysates at 8,000 x g for 5 min at 4°C. Desert the pallets and measure OD260 / OD280 ratio. Balance lysate volume based on OD value then carefully load to the top of sucrose gradients. Centrifuge the gradients at 100,000 x g (23,000 rpm in a SW41 rotor) for 3.5 hrs at 4°C. Collect fractions (avoid any air bubbles) and read OD260 of each fraction.

4.3.4 Subcellular RNA extraction

Cytosolic and nucleic RNAs from cells or tissues are isolated using Norgen Cytoplasmic and Nuclear RNA Purification Kit (Cat. 21000, 37400).

4.3 Results and findings

In TACed mice heart RNA-Seq analysis, we were surprised to identify that translation, including cap-dependent translation, translational initiation, rRNA processing were top related biological processes regulated by Miat (Figure 4-1A). For all ribosomal protein mRNAs differentially expressed between wild type and Miat KO pressure overload mice hearts, wild type hearts show higher RP mRNA expression compared to Miat KO hearts despite the surgery (Figure 4-1B). In Miat KO animals, RPs are even lower expressed after TAC. In NRVMs (Figure 4-1C), mRNAs of RPS6 and RPL6 decreases at baseline when Miat is knockdown, and remain at baseline level under PE 24 hrs treatment while cells express Miat (siNeg) show higher RPs mRNA expression after PE incubation.

We also noted many ribosomal assembly factors were detected in RNA Seq and these genes were lower expressed in Miat KO animals after TAC compared to wild type animals (Figure 4-4A). We examined 45S pre-rRNA, Nxt1 and NOP56 expression by qPCR (Figure 4-4 B-D) in NRVMs and indeed in Miat KD cells, these transcripts are significantly lower upon PE treatment, which suggests Miat might be involved in ribosome biogenesis.

We then examine whether altered RPs mRNA expression in Figure 4-1 could affect protein synthesis in the heart. Figure 4-2 illustrates puromycin labeling we used to track nascent protein synthesis in vivo and in vitro. In NRVMs, Miat KD cells have less protein synthesis rate compared to siNeg transfected cells, and failed to response to PE induced elevated protein synthesis (Figure 4-3A). Consistent with in vitro data, in mouse hearts, Miat KO animals do not present increased protein synthesis upon

PE injection as wild type mice do (Figure 4-3B). In a starving-refeed model which activates mTORC1 activity in induce growth, we observe Miat KO MEFs have lower protein synthesis rate at the baseline and respond to refeed signal at a limited level compared to wild type MEFs (Figure 4-3C), which suggesting Miat functions as a growth signal induced modifier of protein synthesis is not limited to cardiomyocytes.

To further determine how does Miat involve in protein synthesis, especially whether it acts in regulating translation efficiency or translation capacity, we examined the sub cellular localization of Miat. In mouse hearts, Miat is dominantly expressed in the nucleus (Figure 4-5A) as snoU6 presenting positive control of nucleus RNAs. We also show that Miat does not translocate into cytoplasm under TAC induced stress (Figure 4-5B) or PE treatment in NRVMs (Figure 4-5C).

To specifically explore how is ribosome biogenesis is regulated by Miat, we designed probes to detect intermediate rRNAs in ribosome biogenesis process (Figure 4-6). In Miat KO hearts, at baseline (saline injection), there is lower 32S band compared to wild type hearts. 32S decreases in wild type hearts 1hour after PE injection, suggesting rRNAs are processed for ribosome biogenesis purpose while in Miat KO hearts, 32S shows slightly increase after PE injection which indicates accumulation of unprocessed pre-rRNA (Figure 4-7B&C).

Lastly, we used ribosome profiling to check ribosomal subunits and polysome fractions in the cell. In wild type MEF cells, there is a strong enhanced monosome (80S) peak after starve-refeed treatment (red) while Miat KO MEFs do not show increasing ribosome biogenesis activity(purple).

Collectively, our data shows that growth induced ribosome biogenesis at RPs, rRNA, assembly factors and subunits level are all attenuated when Miat is knockout or knockdown, which is strong indication that stress-induced ribosome biogenesis and hypertrophy in the hearts are Miat-dependent.

A

Go terms in biological processes	P-value
SRP-dependent co-translational protein targeting to membrane	4.93e-13
Translational initiation	9.65e-13
Nuclear-transcribed mRNA catabolic process	1.41e-12
Viral transcription	1.71e-10
Translation	3.32e-07
rRNA processing	9.91e-07
Regulation of cell migration	4.32e-06
Angiogenesis	5.70e-06

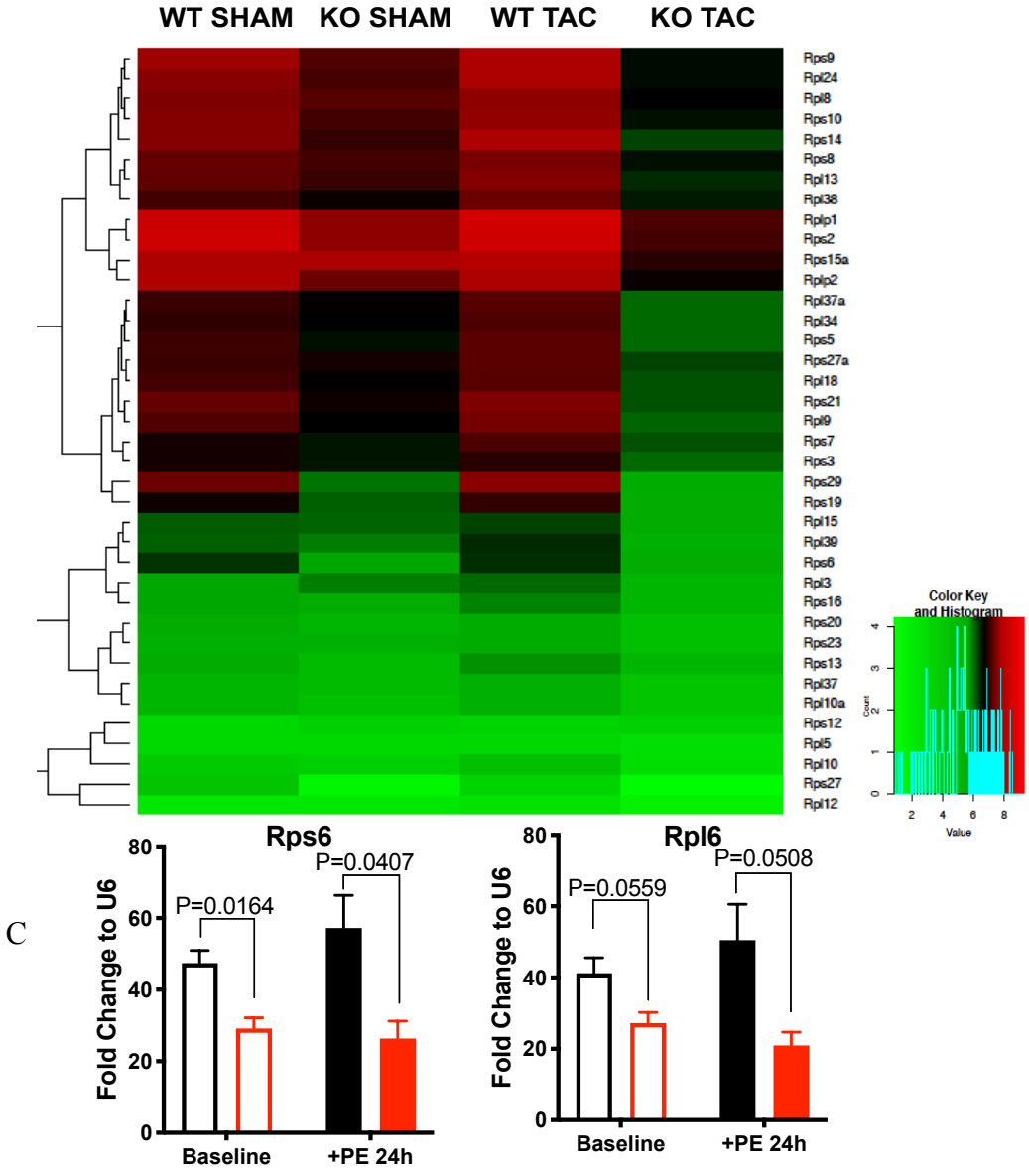

Figure 4-1. Miat regulates ribosomal gene expression in the heart. (A)GO analysis of biological processes in Miat TAC RNA-Seq. Translation related pathways are highlighted in red.(B)mRNA of RPs expression level across four groups as labeled. (C)RPS6 and RPL6 expression detected by qPCR in NRVM cells with SiNeg or SiMiat transfection at baseline or after 24hrs of PE incubation.

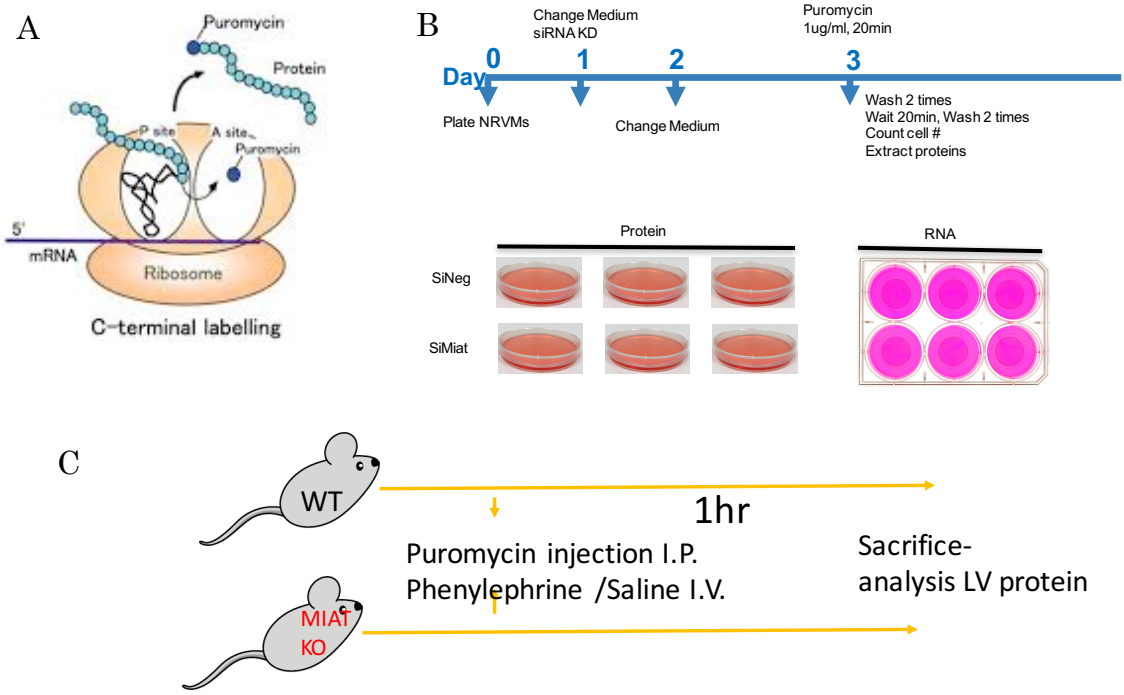

Figure 4-2. Schematic illustration of puromycin labeling assay. (A)Puromycin (dark blue) is incorporated in to polypeptide in translation. (B)Puromycin labeling protocol in NRVMs. Cells are incubated with puromycin to a final concentration of 1ug/ml for 20min before harvest. (C)Puromycin labeling protocol in mouse.

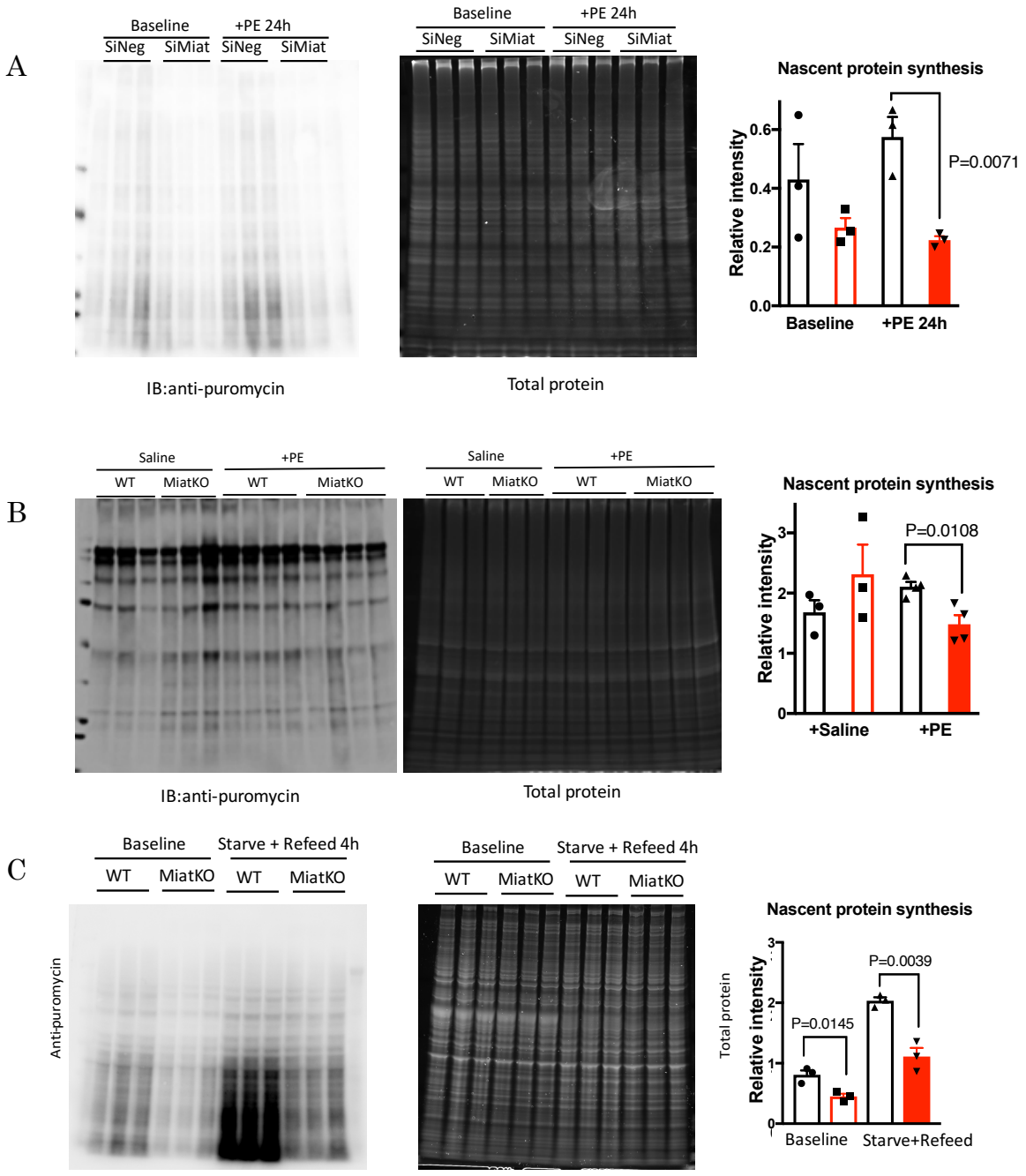

Figure 4-3. Miat is required for elevated protein synthesis. In each panel, puromycin labeling is on the left, total protein stain is in the middle and quantification is on the right. (A)In NRVMs, cells were infected with siNeg control or siMiat knockdown for 48hours, with PE treatment for 24hours before puromycin labeling. (B)In mice, animals received i.p. injection of puromycin and tail vein injection of PE or Saline before tissue collection. (C) In MEF cell, cells were starved with 0.5% FBS for 30 hours before harvest or refeed with 10% FBS for 4 hours before puromycin labeling.

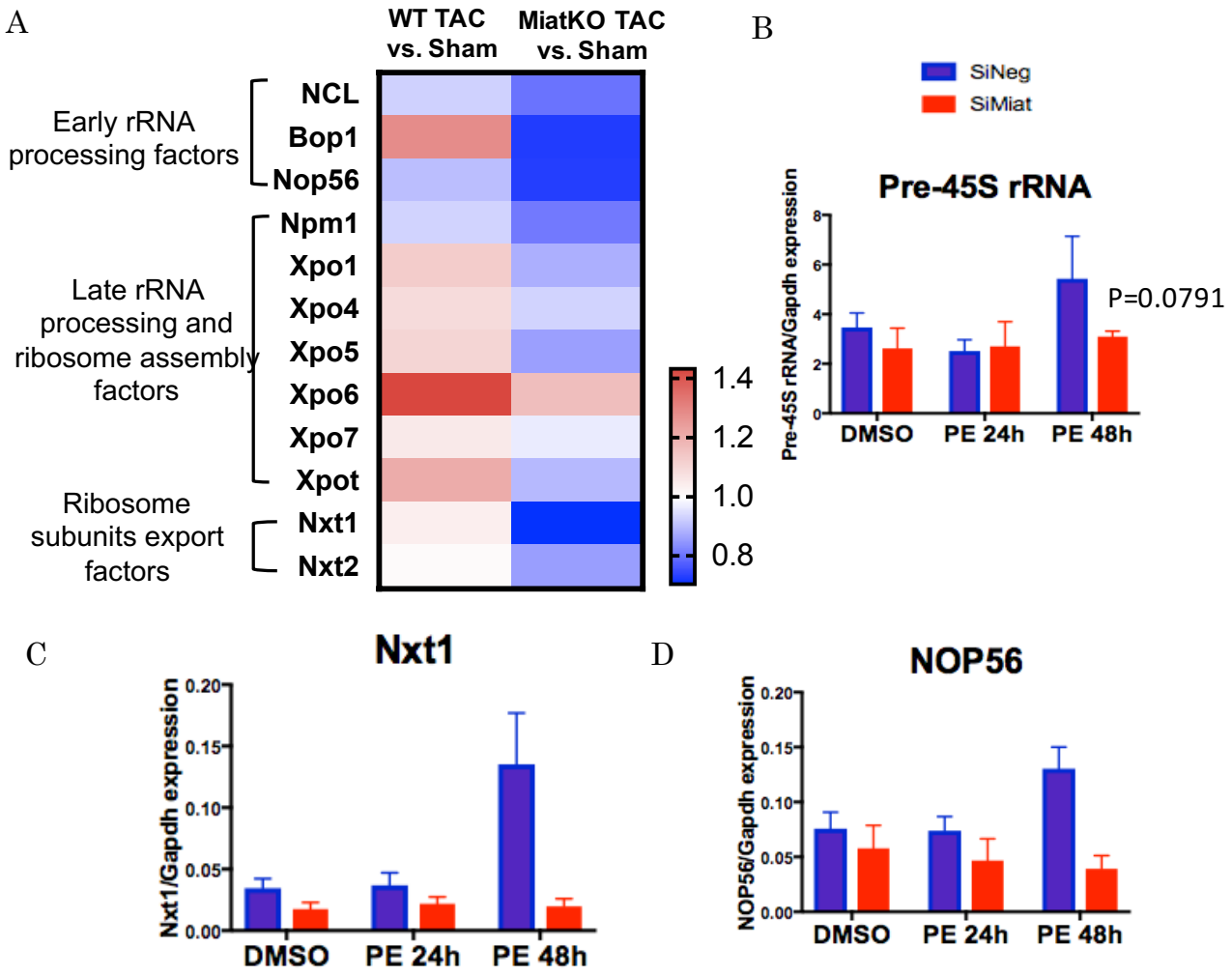

Figure 4-4. Miat regulates ribosome assembly genes and pre-rRNA. (A)Top differentially expressed ribosome assembly factors between wildtype mouse hearts versus Miat KO animals. Genes are grouped based on stages of ribosome assembly. (B)qPCR detects pre-45S RNA level in NRVMs with siNeg (blue bars) and siMiat transfection (red bars) upon DMSO or PE treatment at 24 and 48 hrs. (C)Nxt1 and (D) NOP56 expression in NRVMs as described in (B).

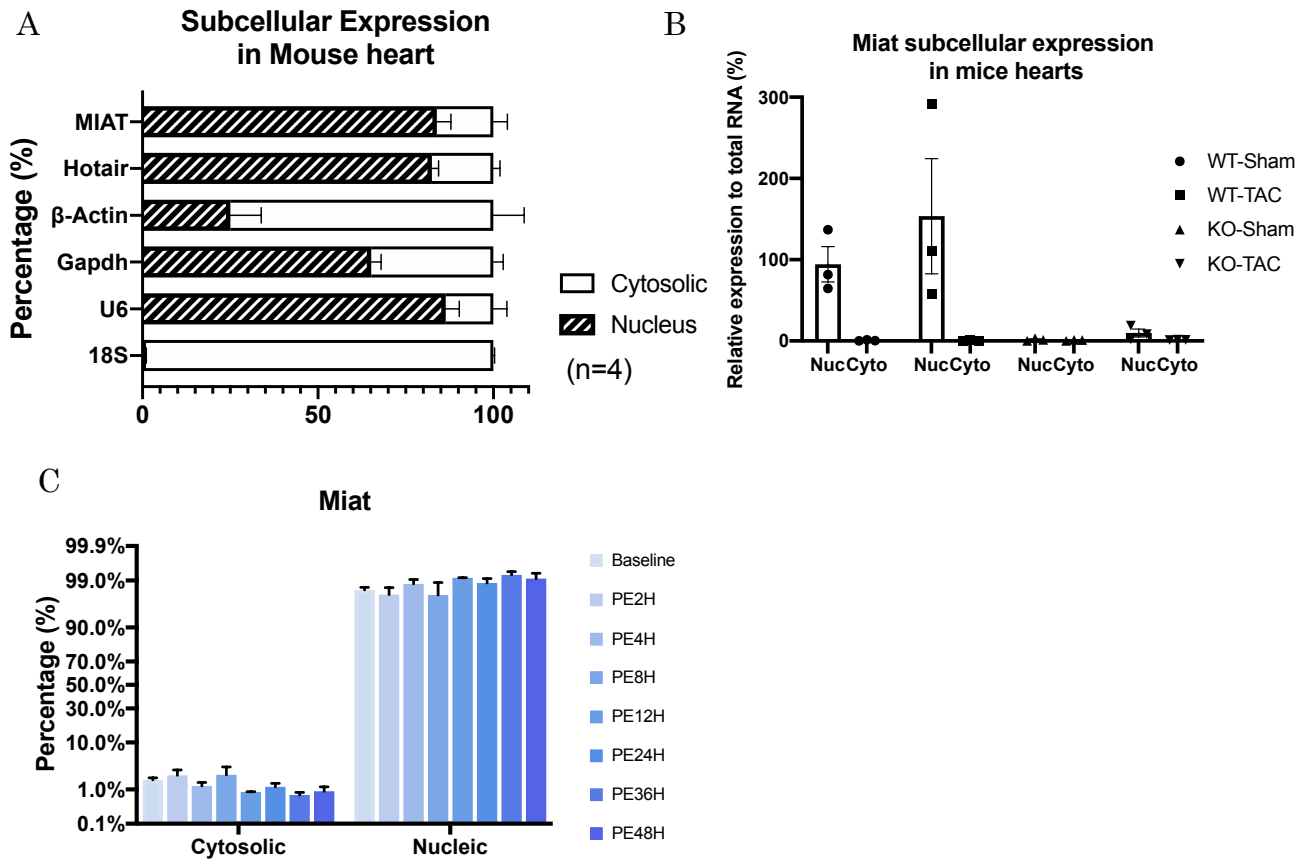

Figure 4-5. Miat dominantly expresses in the nucleus and does not translocate under stress. (A)Subcellular expression of Miat, Hotair, b-Actin, Gapdh, snoU6 and 18S in mouse hearts(n=4). Whole cell expression is balanced to 100% for each RNA. (B)Subcellular expression of Miat in mouse hearts received TAC or Sham treatment. Whole cell expression is balanced to 100%. (C) Subcellular expression of Miat in NRVMs upon PE treatment at baseline, 2hrs, 4hrs, 8hrs, 12hrs, 24hrs, 36hrs and 48hrs. Whole cell expression is balanced to 100%.

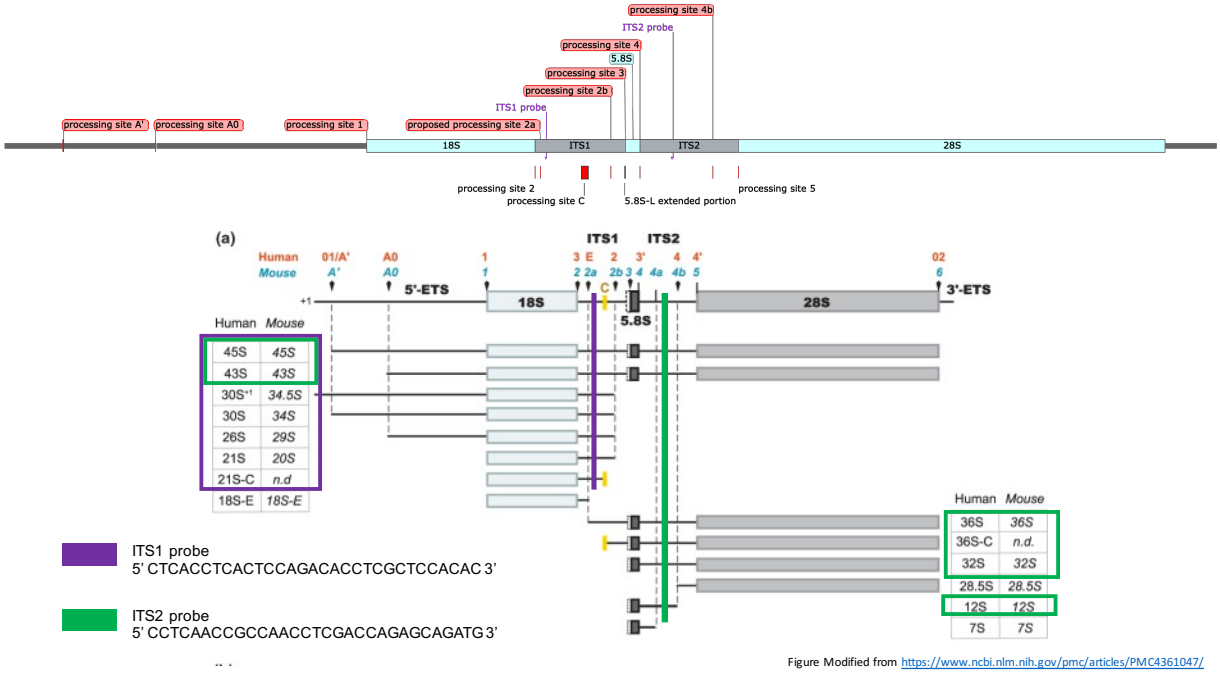

Figure Modified from https://www.ncbi.nlm.nih.gov/pmc/articles/PMC4361047/

Figure 4-6. Design of Northern blotting probes ITS1 and ITS2. Targeted bands are indicated in purple (ITS1) or green (ITS2).

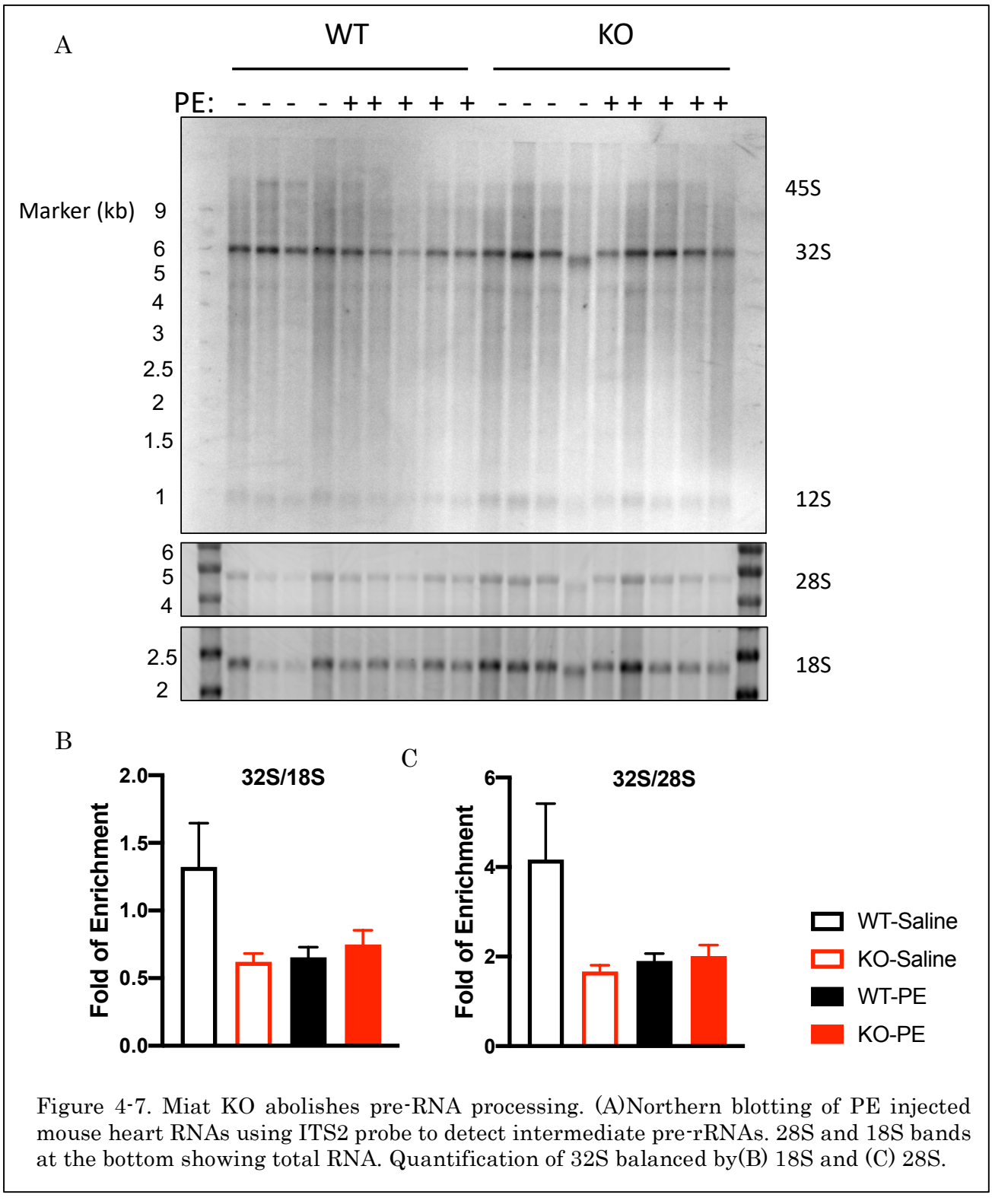

Figure 4-7. Miat KO abolishes pre-RNA processing. (A)Northern blotting of PE injected mouse heart RNAs using ITS2 probe to detect intermediate pre-rRNAs. 28S and 18S bands at the bottom showing total RNA. Quantification of 32S balanced by(B) 18S and (C) 28S.

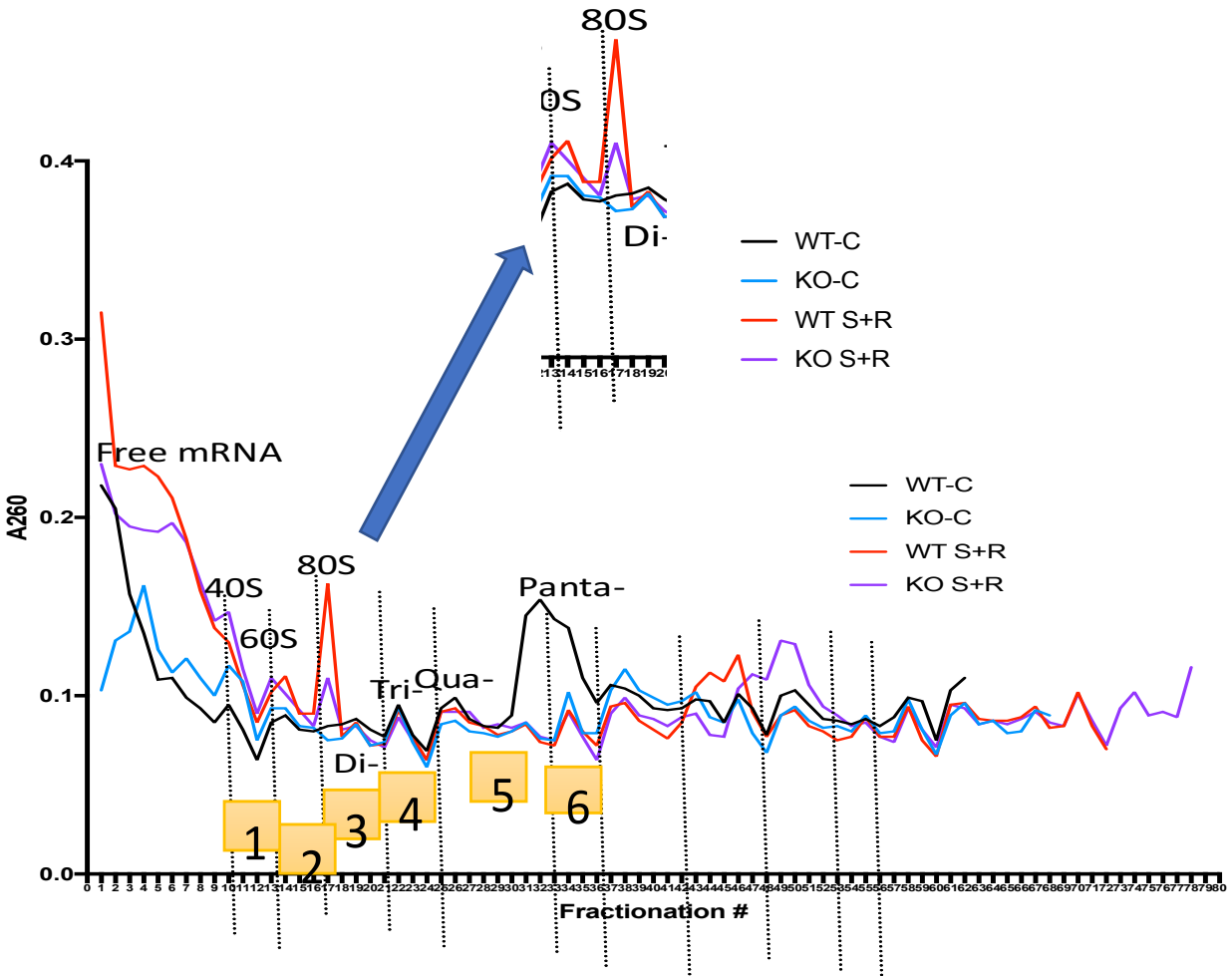

Figure 4-8. Ribosome profiling reveals less ribosomes are assembled under growth in Miat KO MEFs. Cellular lysates from wildtype and MIAT KO MEFs at baseline (WT-C, black and KO-C, blue) and starving-refeed condition (WT S+R, red and KO S+R, purple) were loading to 5%-50% sucrose gradient for fractionation. Free mRNA, 40S, 60S and 80S peaks were labeled with 80S is enlarged.

4.4 Discussion

We used multiple models and assays to explore whether and how does Miat contribute to growth induced protein synthesis in the heart. To our surprise, given the subcellular localization of Miat is dominantly expressed in the nucleus, Miat is likely to regulate protein synthesis on translation capacity rather efficiency where mature ribosomes are in the cytoplasm. We utilized northern blotting to detect rRNA processing, qPCR to detect RP mRNA and ribosome assembly factors, we also showed protein synthesis rate and ribosome profiling data which all consistently indicate that Miat is necessary for growth-induced ribosome biogenesis in the cardiomyocytes. This is the first stress-responsive lncRNA to data that has been recognized to specially regulates ribosome biogenesis in cardiac hypertrophy.

Acknowledgements

We would like to thank Dr. Jonelle White from Dr. Steve Clarke's lab of biochemistry department at UCLA for their help on ribosome profiling. We thank Samantha Edwards from Dr. Tracey Johnson's lab of Molecular, Cell & Developmental Biology department at UCLA for their help of Northern blotting.

CHAPTER V. MIAT BINDS TO NUCLEOLIN AND REGULATES PROTEIN SYNTHESIS AND NUCLEOLI FORMATION IN CARDIOMYOCYTES

5.1 Introduction

To further explore which steps of ribosome biogenesis does Miat contribute to, we searched for the binding partners of Miat. In this chapter, we show that Miat binds to nucleolus protein nucleolin and such binding is necessary for NCL mediated rRNA process and ribosome biogenesis. Moreover, we also show that Miat-NCL interaction is required for protein synthesis and nucleoli formation in cardiomyocytes.

5.2 Methods and materials

RNA immunoprecipitation(RIP)

The RIP assay was done by Magna RIP™ RNA-Binding Protein Immunoprecipitation Kit from Sigma (Cat 17-700) per manufacture's protocol. For each RIP, we prepared $5x10^6$ cells to lysate and used 5% lysate as input.

5.3 Results and findings

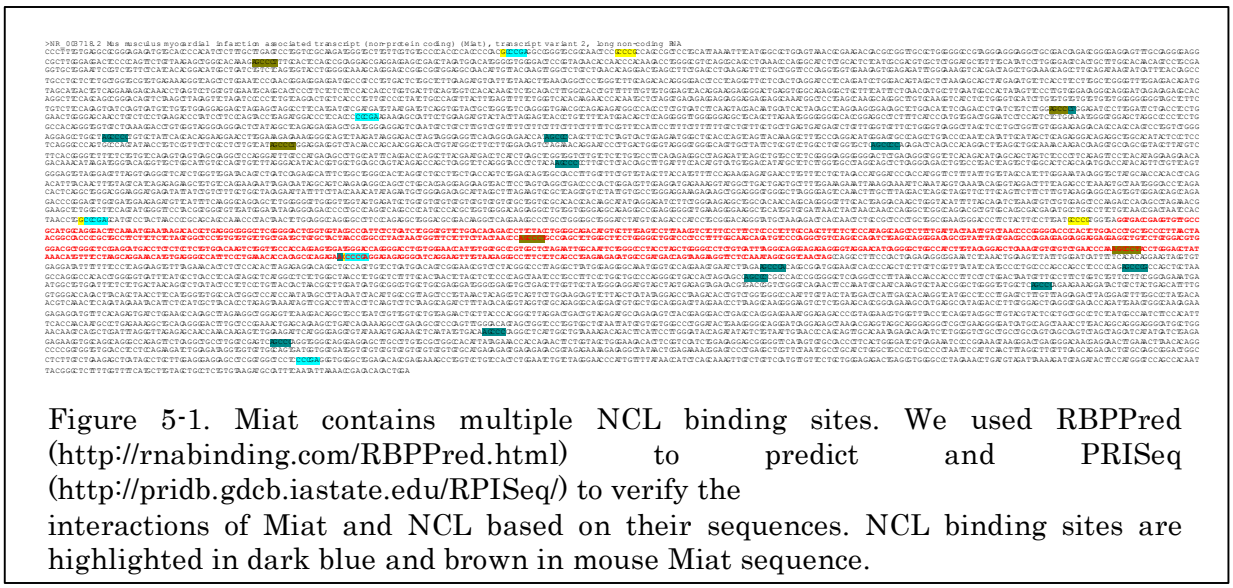

Figure 5-1. Miat contains multiple NCL binding sites. We used RBPPred (http://rnabinding.com/RBPPred.html) to predict and PRISeq (http://pridb.gdcb.iastate.edu/RPISeq/) to verify the interactions of Miat and NCL based on their sequences. NCL binding sites are highlighted in dark blue and brown in mouse Miat sequence.

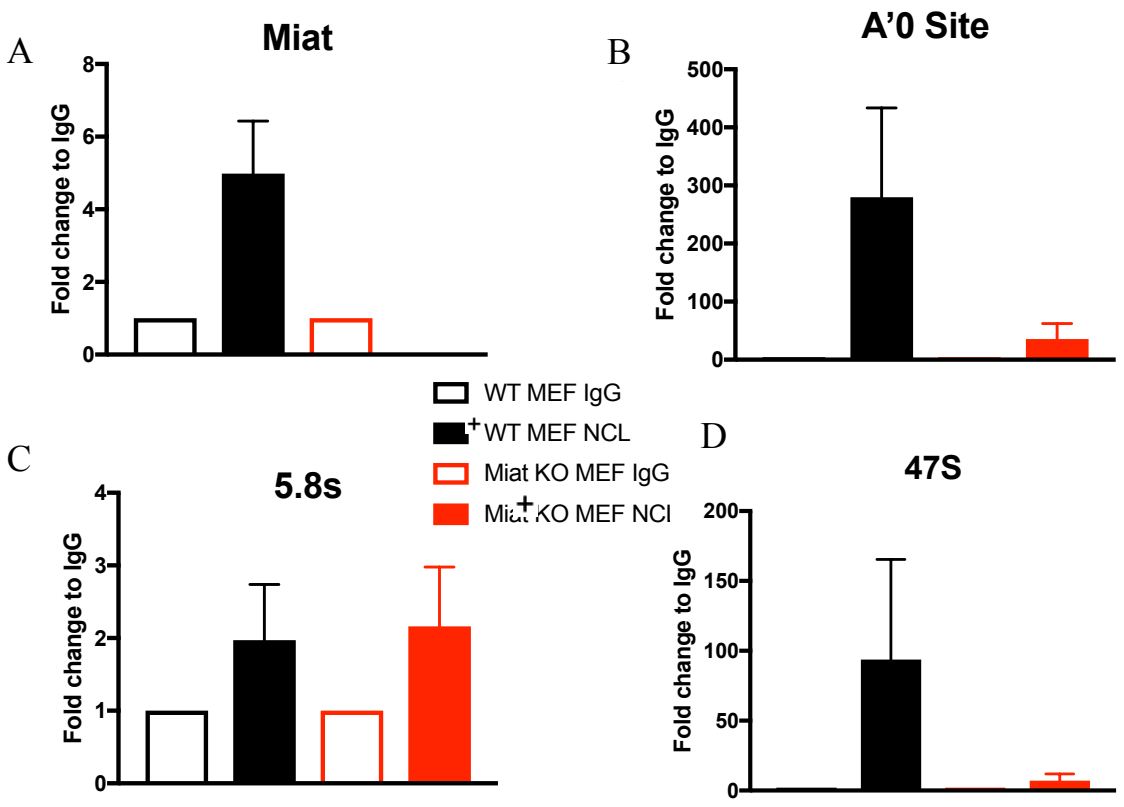

Figure 5-2. Miat binds to NCL and is required for NCL-pre-rRNA binding. In MEF cells, we detect Miat-NCL binding using NCL specific antibody with IgG as control. (A)Miat has a 5-fold affinity to NCL compared to IgG and such enrichment was not observed in Miat KO MEFs (in read). (B)A'0 processing site of 47S pre-rRNA showed over 250-fold enrichment to bind to NCL compared to IgG but the level drops to less than 40 when Miat is knockout. (C)5.8S rRNA did not show affinity to NCL in both wildtype MEF and Miat KO MEFs. (D) 47S pre-rRNA binds to NCL with an 80-fold enrichment but not in Miat.

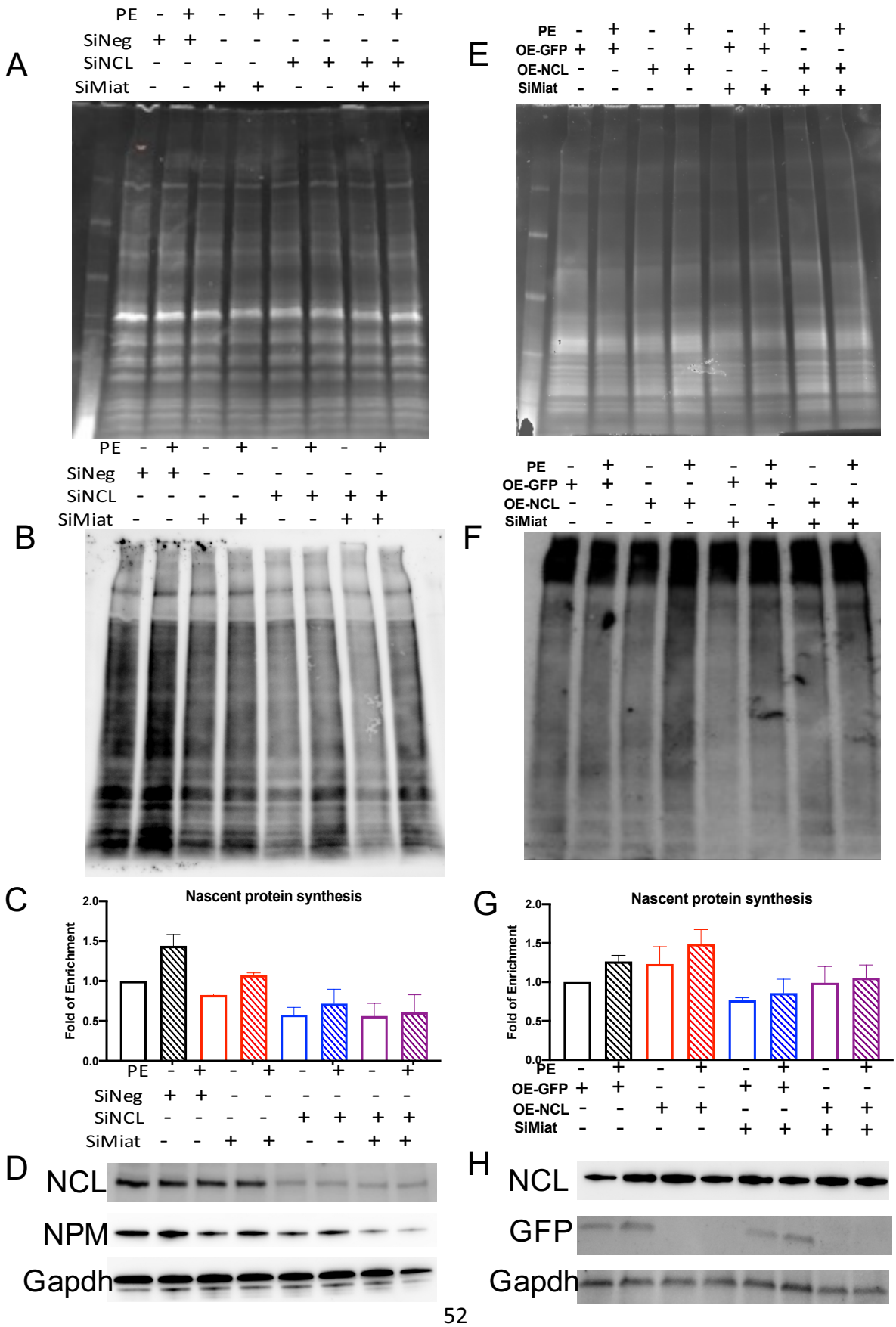
A
PE - + - + - + - +
SiNeg + + - - - - - -
SiNCL - - - - + + + +
SiMiat - - + + - - + +
B
PE - + - + - + - +
SiNeg + + - - - - - -
SiNCL - - - - + + + +
SiMiat - - + + - - + +
C
Nascent protein synthesis
Fold of Enrichment
2.0
1.5
1.0
0.5
0.0
PE - + - + - + - +
SiNeg + + - - - - - -
SiNCL - - - - + + + +
SiMiat - - + + - - + +
D
NCL
NPM
Gapdh
E
PE - + - + - + - +
OE-GFP + + - - + + - -
OE-NCL - - + + - - + +
SiMiat - - - - + + + +
F
PE - + - + - + - +
OE-GFP + + - - + + - -
OE-NCL - - + + - - + +
SiMiat - - - - + + + +
G
Nascent protein synthesis
Fold of Enrichment
2.0
1.5
1.0
0.5
0.0
PE - + - + - + - +
OE-GFP + + - - + + - -
OE-NCL - - + + - - + +
SiMiat - - - - + + + +
H
NCL
GFP
Gapdh

Figure 5-3 Miat-NCL interaction mediates protein synthesis in cardiomyocytes synergistically. (A)Total protein as input in NCL and Miat knockdown groups of NRVMs. (B)puromycin labeling of protein synthesis across KD groups with/without PE stimuli. (C)quantification of panel (B) using (A) as input balance of each lane. (D)western blotting showing knockdown efficiency of NCL. (E)total protein input for NCL overexpression in NRVMs. (F)puromycin labeling of protein synthesis in NCL OE groups. (G)quantification of panel (F) with (E) as balance. (H)western blotting to verify overexpression of NCL and GFP.

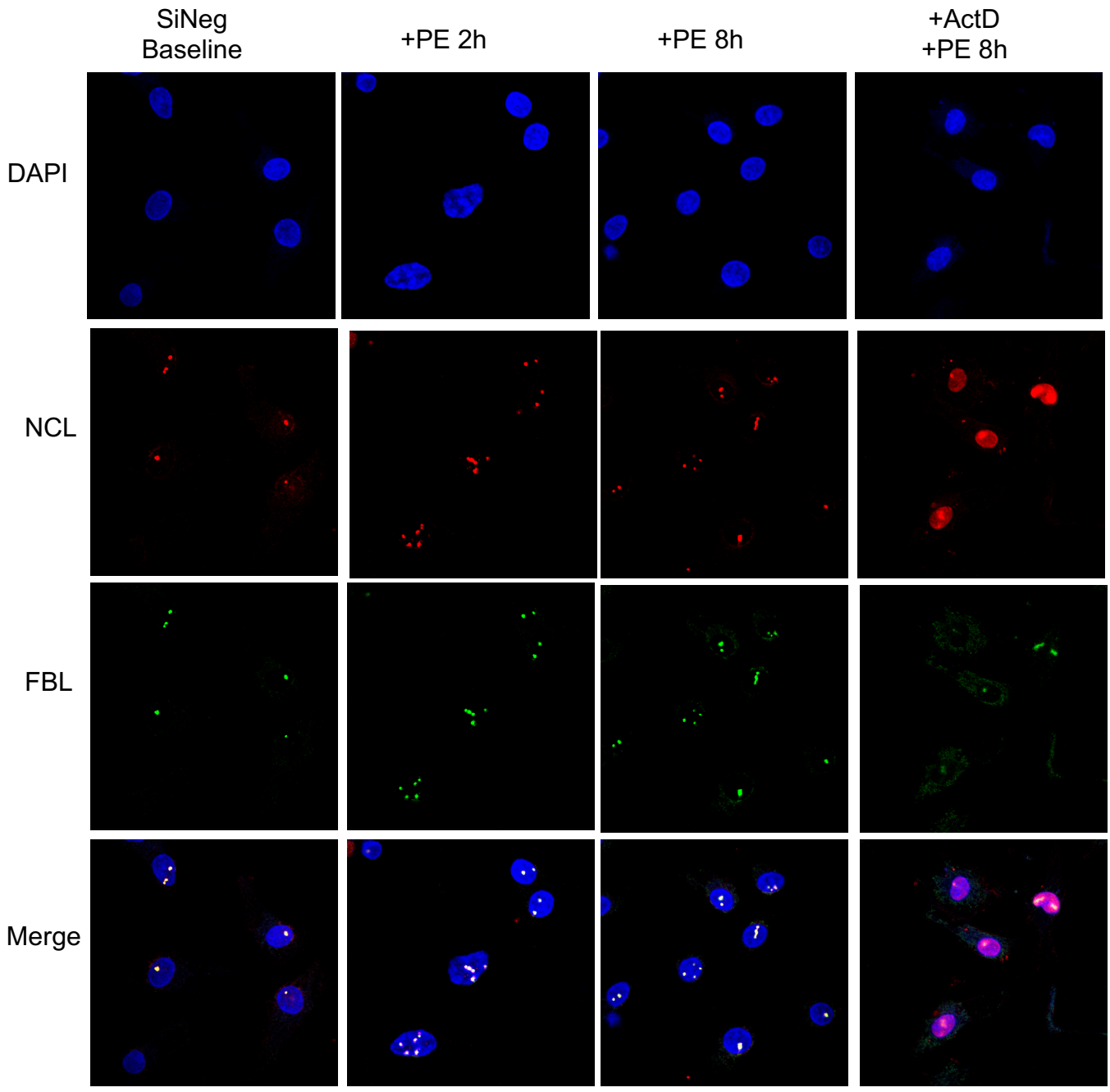

Figure 5-4 PE induces nucleoli formation in NRVMs. NRVMs transfected with siNeg for 48hours with no (baseline), 2hrs, 8hrs PE treatment and 8hrs PE treatment plus 2hours of ActD are stained with DAPI(blue), NCL(red), FBL(green).

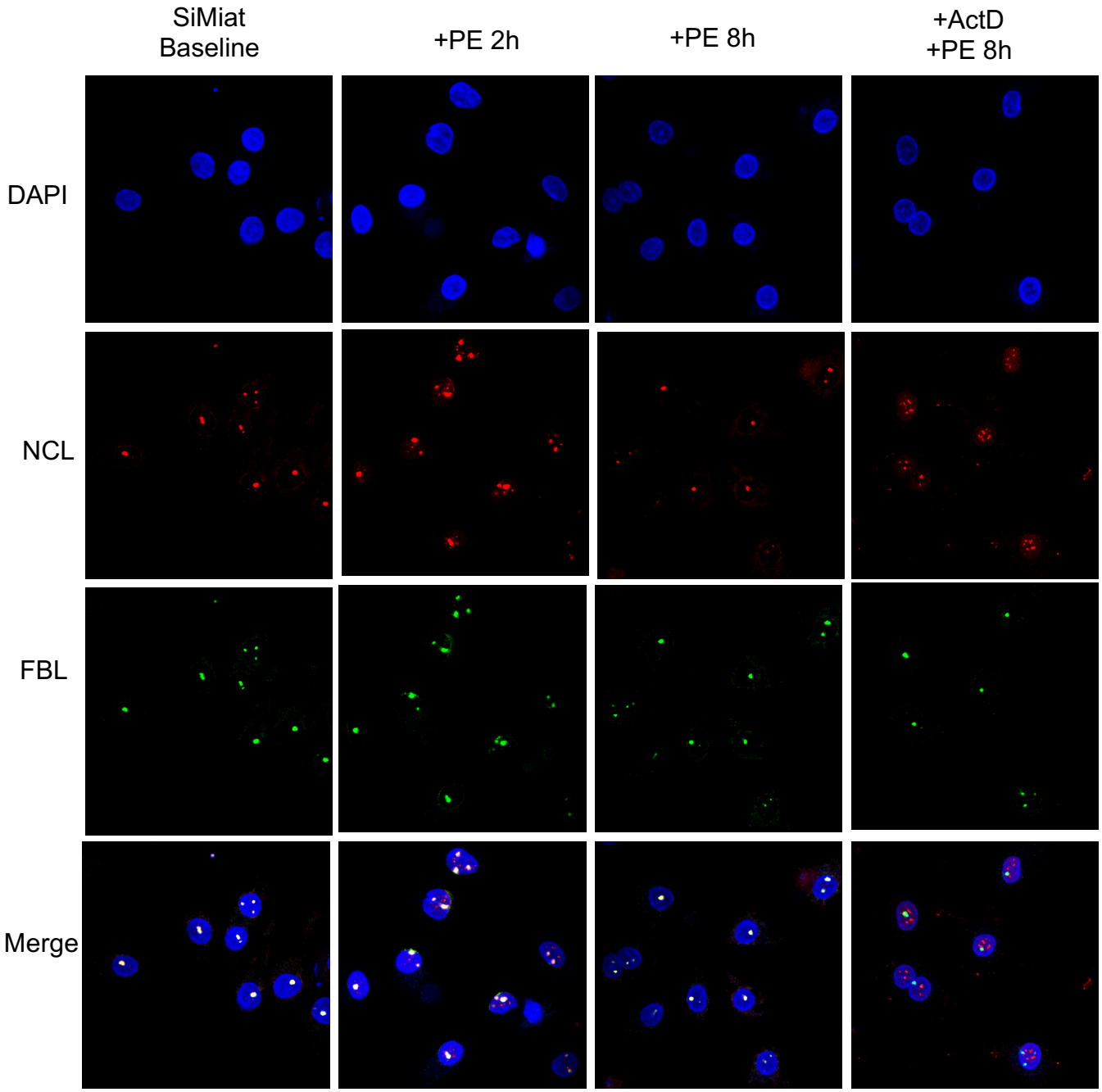

Figure 5-5. PE induces nucleoli formation in NRVMs is Miat dependent. NRVMs transfected with siMiat for 48hours with no (baseline), 2hrs, 8hrs PE treatment and 8hrs PE treatment plus 2hours of ActD are stained with DAPI(blue), NCL(red), FBL(green).

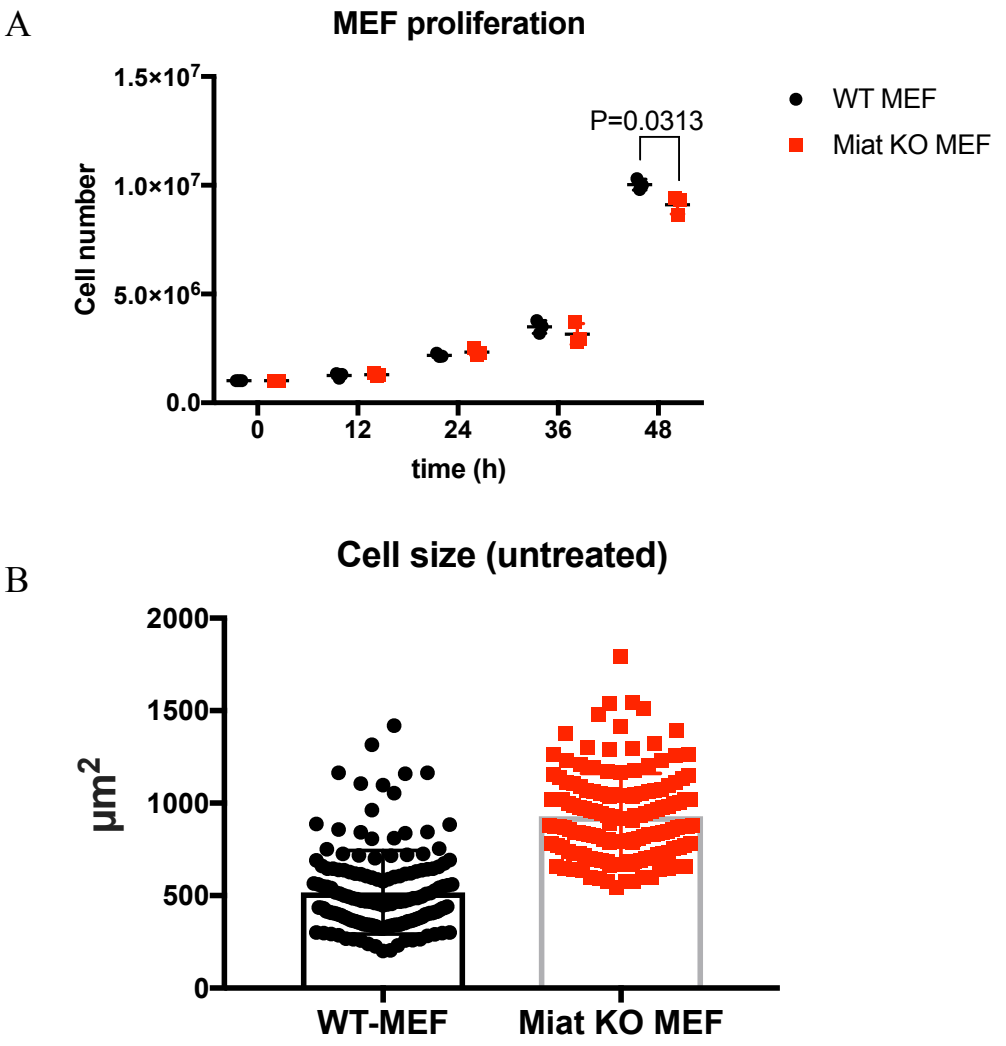

Figure 5-6. Miat is required to maintain cell cycle and cell size in MEF. (A) Cell numbers of wildtype MEF(black) and Miat KO MEF(red) are measured over time from plating (0) to 48 hours. (B) Cell sizes of wildtype MEF and Miat KO MEF under 10%FBS culture condition.

We first use bioinformatics tools RBPPred and PRISeq to predict which proteins might bind to Miat with following screening criteria: (1) Miat contains protein binding motif in its sequence; (2)the protein expresses in heart; (3)protein predominantly expresses in the nucleus; (4) functional relevance to Miat. NCL was the most promising candidate protein (Figure 5-1). We verified their binding using RIP assay

(Figure 5-2). Miat shows a 5-fold enrichment binding to NCL compare to IgG and the binding is lost in Miat KO cells (Figure 5-2A). 47S is known to bind to NCL and was used as positive control in the assay and indeed it has a ~80-fold binding affinity compared to IgG (Figure 5-2D), its A'0 processing site shows a even higher affinity to NCL with a ~250-fold increase compare to IgG (Figure 5-2B). To our surprise, in Miat KO cells, NCL does not bind to 47S or A'0 site suggesting the interaction between NCL and pre-rRNA is Miat dependent. Mature 5.8S is used as a negative control which does not bind to NCL and is not mediated by Miat (Figure 5-2C).

We then examined whether Miat-NCL interaction regulates protein synthesis in the cardiomyocytes. In NRVMs, we did gain-of-function and loss-of-function assays to manipulate Miat and NCL expression, and used puromycin labeled nascent protein synthesis as readout. We show that when Miat is knockdown, protein synthesis drops by ~30% in NRVMs, and when NCL is knockdown, protein synthesis rate drops even more by ~50%. When both Miat and NCL is knockdown, protein synthesis is down-regulated by ~50%, which is similar to NCL knockdown groups. In all Miat and NCL knockdown conditions, we observed that cardiomyocytes do not respond well to PE stimulation well whereas the control cells received siNeg shows a ~30% induced protein synthesis (Figure 5-3A-D). However, when NCL is over expressed in the cardiomyocytes, protein synthesis is up-regulated by ~20% despite the over expression level is mild (Figure 5-3H). More importantly, such enhanced protein synthesis mediated by NCL over expression is Miat dependent as in Miat KD cardiomyocytes, protein synthesis is back to baseline level and response less to PE stimulation (Figure 5-3 F, G, H).

Nucleolus is the birthplace of ribosomes and where NCL dominantly expressed as we discussed in Chapter I and III, so we checked how is nucleus is regulated by Miat. In NRVMs, we stained cells with NCL and FBL under siNeg or siMiat conditions. We used PE to treat the cells to induce ribosome biogenesis and Actmyocin D as an inhibitor of ribosome biogenesis. In Figure 5-4, we show that upon PE stimulation, more nucleoli are formed in cardiomyocytes. With ActD inhibition, both NCL and FBL are diffused into nucleus and the nucleoli are disassembled. However, when Miat is knockdown, we see NCL does not co-localize well with FBL to form functional nucleoli, but rather scattered in the nucleus. With ActD inhibition, most of NCL expression is scattered without co-localize with FBL in the nucleoli (Figure 5-5). This suggests that Miat is required for new nucleoli formation in the cardiomyocytes under hypertrophic stimulation.

In cell types that proliferate, the nucleolus undergoes assembly and dismiss during cell cycle. In the MEFs, we observed Miat KO MEFs are less proliferative compared to wild type cells (Figure 5-6A) with an enlarged cell size (Figure 5-6B) which suggests Miat mediated nucleoli formation may not be limited to cardiomyocytes, but to proliferative cells as well.

5.4 Discussion

In this chapter, we established the binding between Miat and NCL and showed that such binding is essential for 1) NCL mediated pre-rRNA processing and 2) enhanced protein synthesis driven by NCL overexpression. Double knockdown of Miat and NCL shows similar down-regulation of protein synthesis rate in cardiomyocytes while in Miat KD cells the NCL induced protein synthesis was gone suggesting they two work

synergistically. We also explored nucleoli formation in cardiomyocytes under hypertrophic stimuli and how is that regulated by Miat and NCL interaction. Strikingly, unlike cancer cells which typically enlarge nucleoli size to allow more ribosome biogenesis, cardiomyocytes form more nucleoli to adapt to growing need of ribosome assembly. We showed that under PE treatment, as early as 2hours post stimulation, more nucleoli are formed in the cells and this phenomenon is Miat dependent. We also show when Miat is knockdown, NCL fails to co-localize with FBL to form functional nucleoli. These findings for the first time revealed how nucleoli contributes to hypertrophy of cardiomyocytes and how important a lncRNA is in early response to the process.

Acknowledgements

We thank Fangtao Chi from Dr. Utpal Banerjee lab at UCLA for his advice on confocal imaging and UCLA Broad Stem Cell Research Center (BSCRC) for providing access to the confocal core.

CHAPTER VI. SUMMARY

6.1 Working model

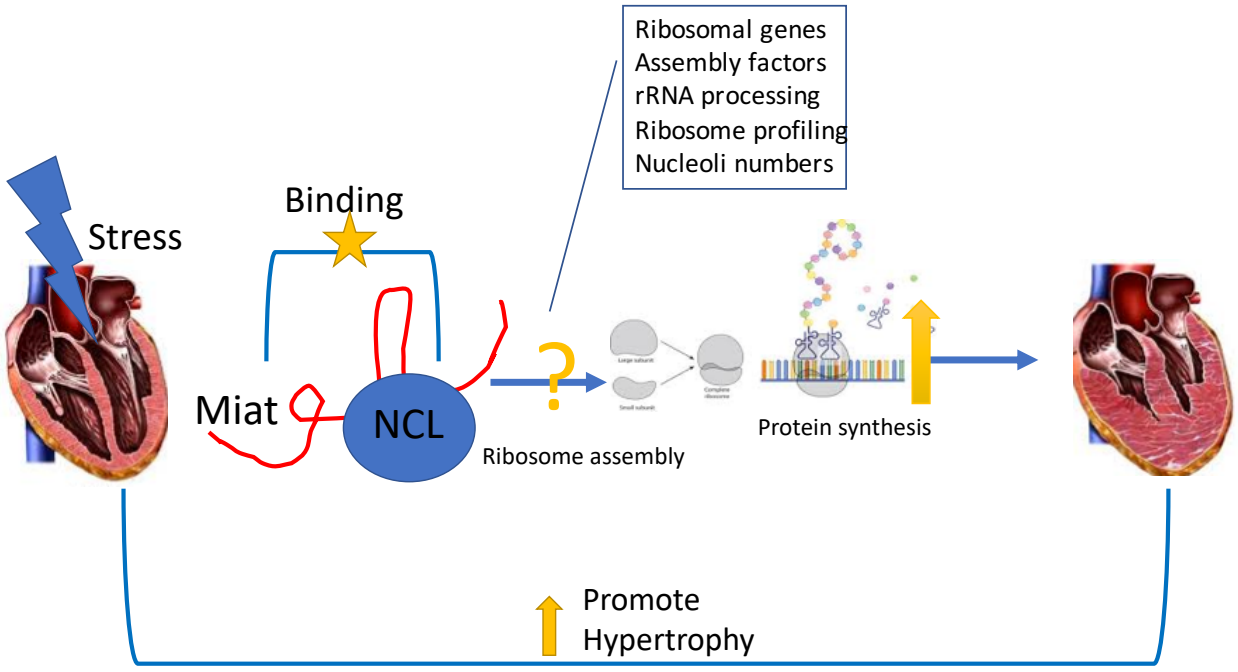

In this thesis, we identified a lncRNA Miat responses to hypertrophic stimulation in the heart and is necessary for cardiac hypertrophy *in vitro* and *in vivo*. In Miat KO animals, the hearts are more resistant to TAC or drug induced hypertrophy with normal baseline functions. Mechanistically, we show that Miat regulates ribosomal gene expression and assembly factors in the cardiomyocytes to affect stress induced protein synthesis. Moreover, Miat binds to NCL and is required for NCL mediated pre-rRNA assembly, nucleoli formation and ribosome biogenesis in the heart. These findings give a specific example of how gene expression is regulated at translational capacity level in cardiac hypotrophy.

6.2 Future perspectives

Miat-NCL interaction is essential for ribosome biogenesis under hypertrophic stimuli in the cardiomyocytes, our findings trigger more questions to ask about the translational regulation in the hypertrophic heart. Here are several directions to consider: first, does the same mechanism apply to physiological hypertrophy? Second, is it possible to tune the protein synthesis rate by manipulate Miat-NCL binding? Or further, could blocking of Miat-NCL interaction be a target of treating pathological cardiac hypertrophy? We also do not know yet which specific rRNA processing steps or ribosome assembly steps are regulated Miat. Addressing these questions will greatly enhance our current understanding of ribosome biogenesis and cardiac-specific translational regulation.

REFERENCE

1. Pontvianne F, Abou-Ellail M, Douet J, Comella P, Matia I, Chandrasekhara C, Debures A, Blevins T, Cooke R, Medina FJ, Tourmente S, Pikaard CS, Saez-Vasquez J. Nucleolin is required for DNA methylation state and the expression of rRNA gene variants in Arabidopsis thaliana. PLoS Genet. 2010;6(11):e1001225. Epub 2010/12/03. doi: 10.1371/journal.pgen.1001225. PubMed PMID: 21124873; PMCID: PMC2991258.
2. Durut N, Saez-Vasquez J. Nucleolin: dual roles in rDNA chromatin transcription. Gene. 2015;556(1):7-12. Epub 2014/09/17. doi: 10.1016/j.gene.2014.09.023. PubMed PMID: 25225127.
3. Kressler D, Hurt E, Bassler J. A Puzzle of Life: Crafting Ribosomal Subunits. Trends Biochem Sci. 2017;42(8):640-54. Epub 2017/06/06. doi: 10.1016/j.tibs.2017.05.005. PubMed PMID: 28579196.
4. Scott DD, Oeffinger M. Nucleolin and nucleophosmin: nucleolar proteins with multiple functions in DNA repair. Biochem Cell Biol. 2016;94(5):419-32. Epub 2016/09/28. doi: 10.1139/bcb-2016-0068. PubMed PMID: 27673355.
5. Farley-Barnes KI, McCann KL, Ogawa LM, Merkel J, Surovtseva YV, Baserga SJ. Diverse Regulators of Human Ribosome Biogenesis Discovered by Changes in Nucleolar Number. Cell Rep. 2018;22(7):1923-34. Epub 2018/02/15. doi: 10.1016/j.celrep.2018.01.056. PubMed PMID: 29444442; PMCID: PMC5828527.
6. Morgan HE, Siehl D, Chua BH, Lautensack-Belser N. Faster protein and ribosome synthesis in hypertrophying heart. Basic Res Cardiol. 1985;80 Suppl 2:115-8. Epub 1985/01/01. PubMed PMID: 2415104.
7. Nagai R, Low RB, Stirewalt WS, Alpert NR, Litten RZ. Efficiency and capacity of protein synthesis are increased in pressure overload cardiac hypertrophy. Am J Physiol. 1988;255(2 Pt 2):H325-8. Epub 1988/08/01. doi: 10.1152/ajpheart.1988.255.2.H325. PubMed PMID: 2457329.
8. Morgan HE, Beinlich CJ. Contributions of increased efficiency and capacity of protein synthesis to rapid cardiac growth. Mol Cell Biochem. 1997;176(1-2):145-51. Epub 1997/12/24. PubMed PMID: 9406156.
9. Hannan RD, Jenkins A, Jenkins AK, Brandenburger Y. Cardiac hypertrophy: a matter of translation. Clin Exp Pharmacol Physiol. 2003;30(8):517-27. Epub 2003/08/02. PubMed PMID: 12890171.
10. Escobar J, Frank JW, Suryawan A, Nguyen HV, Kimball SR, Jefferson LS, Davis TA. Regulation of cardiac and skeletal muscle protein synthesis by individual branched-chain amino acids in neonatal pigs. Am J Physiol Endocrinol Metab. 2006;290(4):E612-21. Epub 2005/11/10. doi: 10.1152/ajpendo.00402.2005. PubMed PMID: 16278252.
11. Heineke J, Molkentin JD. Regulation of cardiac hypertrophy by intracellular signalling pathways. Nat Rev Mol Cell Biol. 2006;7(8):589-600. doi: 10.1038/nrm1983. PubMed PMID: 16936699.
12. Sinex FM, Macmullen J, Hastings AB. The effect of insulin on the incorporation of C14 into the protein of rat diaphragm. J Biol Chem. 1952;198(2):615-9. Epub 1952/10/01. PubMed PMID: 12999777.
13. Hobuss L, Bar C, Thum T. Long Non-coding RNAs: At the Heart of Cardiac Dysfunction? Front Physiol. 2019;10:30. Epub 2019/02/15. doi: 10.3389/fphys.2019.00030. PubMed PMID: 30761015; PMCID: PMC6361744.

14. Henras AK, Plisson-Chastang C, O'Donohue MF, Chakraborty A, Gleizes PE. An overview of pre-ribosomal RNA processing in eukaryotes. Wiley Interdiscip Rev RNA. 2015;6(2):225-42. doi: 10.1002/wrna.1269. PubMed PMID: 25346433; PMCID: PMC4361047.
15. Ivester CT, Tuxworth WJ, Cooper Gt, McDermott PJ. Contraction accelerates myosin heavy chain synthesis rates in adult cardiocytes by an increase in the rate of translational initiation. J Biol Chem. 1995;270(37):21950-7. Epub 1995/09/15. doi: 10.1074/jbc.270.37.21950. PubMed PMID: 7665617.
16. Wada H, Ivester CT, Carabello BA, Cooper Gt, McDermott PJ. Translational initiation factor eIF-4E. A link between cardiac load and protein synthesis. J Biol Chem. 1996;271(14):8359-64. Epub 1996/04/05. doi: 10.1074/jbc.271.14.8359. PubMed PMID: 8626533.
17. Beinlich CJ, Rissinger CJ, Morgan HE. Mechanisms of rapid growth in the neonatal pig heart. J Mol Cell Cardiol. 1995;27(1):273-81. Epub 1995/01/01. doi: 10.1016/s0022-2828(08)80026-0. PubMed PMID: 7760351.
18. Tafforeau L, Zorbas C, Langhendries JL, Mullineux ST, Stamatopoulou V, Mullier R, Wacheul L, Lafontaine DL. The complexity of human ribosome biogenesis revealed by systematic nucleolar screening of Pre-rRNA processing factors. Mol Cell. 2013;51(4):539-51. Epub 2013/08/27. doi: 10.1016/j.molcel.2013.08.011. PubMed PMID: 23973377.
19. Powers T. Ribosome biogenesis: giant steps for a giant problem. Cell. 2004;119(7):901-2. Epub 2004/12/29. doi: 10.1016/j.cell.2004.12.011. PubMed PMID: 15620347.
20. Ginisty H, Amalric F, Bouvet P. Nucleolin functions in the first step of ribosomal RNA processing. EMBO J. 1998;17(5):1476-86. Epub 1998/04/18. doi: 10.1093/emboj/17.5.1476. PubMed PMID: 9482744; PMCID: PMC1170495.
21. Bouvet P, Diaz JJ, Kindbeiter K, Madjar JJ, Amalric F. Nucleolin interacts with several ribosomal proteins through its RGG domain. J Biol Chem. 1998;273(30):19025-9. Epub 1998/07/21. doi: 10.1074/jbc.273.30.19025. PubMed PMID: 9668083.
22. Benjamin EJ, Muntner P, Alonso A, Bittencourt MS, Callaway CW, Carson AP, Chamberlain AM, Chang AR, Cheng S, Das SR, Delling FN, Djousse L, Elkind MSV, Ferguson JF, Fornage M, Jordan LC, Khan SS, Kissela BM, Knutson KL, Kwan TW, Lackland DT, Lewis TT, Lichtman JH, Longenecker CT, Loop MS, Lutsey PL, Martin SS, Matsushita K, Moran AE, Mussolino ME, O'Flaherty M, Pandey A, Perak AM, Rosamond WD, Roth GA, Sampson UKA, Satou GM, Schroeder EB, Shah SH, Spartano NL, Stokes A, Tirschwell DL, Tsao CW, Turakhia MP, VanWagner LB, Wilkins JT, Wong SS, Virani SS, American Heart Association Council on E, Prevention Statistics C, Stroke Statistics S. Heart Disease and Stroke Statistics-2019 Update: A Report From the American Heart Association. Circulation. 2019;139(10):e56-e528. Epub 2019/02/01. doi: 10.1161/CIR.0000000000000659. PubMed PMID: 30700139.
23. Sayed D, He M, Yang Z, Lin L, Abdellatif M. Transcriptional regulation patterns revealed by high resolution chromatin immunoprecipitation during cardiac hypertrophy. J Biol Chem. 2013;288(4):2546-58. Epub 2012/12/12. doi: 10.1074/jbc.M112.429449. PubMed PMID: 23229551; PMCID: PMC3554922.
24. Karbassi E, Rosa-Garrido M, Chapski DJ, Wu Y, Ren S, Wang Y, Stefani E, Vondriska TM. Direct visualization of cardiac transcription factories reveals regulatory principles of nuclear architecture during pathological remodeling. J Mol Cell Cardiol. 2019;128:198-211. Epub 2019/02/12. doi: 10.1016/j.yjmcc.2019.02.003. PubMed PMID: 30742811; PMCID: PMC6644685.

25. Xiao D, Dasgupta C, Chen M, Zhang K, Buchholz J, Xu Z, Zhang L. Inhibition of DNA methylation reverses norepinephrine-induced cardiac hypertrophy in rats. Cardiovasc Res. 2014;101(3):373-82. Epub 2013/11/26. doi: 10.1093/cvr/cvt264. PubMed PMID: 24272874; PMCID: PMC3927999.
26. Liu L, He X, Zhao M, Yang S, Wang S, Yu X, Liu J, Zang W. Regulation of DNA methylation and 2-OG/TET signaling by choline alleviated cardiac hypertrophy in spontaneously hypertensive rats. J Mol Cell Cardiol. 2019;128:26-37. Epub 2019/01/21. doi: 10.1016/j.yjmcc.2019.01.011. PubMed PMID: 30660679.
27. Zhang L, Hamad EA, Vausort M, Funakoshi H, Nicot N, Nazarov PV, Vallar L, Feldman AM, Wagner DR, Devaux Y, Cardiolinc n. Whole transcriptome microarrays identify long non-coding RNAs associated with cardiac hypertrophy. Genom Data. 2015;5:68-71. Epub 2015/10/21. doi: 10.1016/j.gdata.2015.05.014. PubMed PMID: 26484228; PMCID: PMC4583629.
28. Gao C, Ren S, Lee JH, Qiu J, Chapski DJ, Rau CD, Zhou Y, Abdellatif M, Nakano A, Vondriska TM, Xiao X, Fu XD, Chen JN, Wang Y. RBFox1-mediated RNA splicing regulates cardiac hypertrophy and heart failure. J Clin Invest. 2016;126(1):195-206. Epub 2015/12/01. doi: 10.1172/JCI84015. PubMed PMID: 26619120; PMCID: PMC4701548.
29. Streicher JM, Ren S, Herschman H, Wang Y. MAPK-activated protein kinase-2 in cardiac hypertrophy and cyclooxygenase-2 regulation in heart. Circ Res. 2010;106(8):1434-43. Epub 2010/03/27. doi: 10.1161/CIRCRESAHA.109.213199. PubMed PMID: 20339119; PMCID: PMC2903446.
30. Chowdhury D, Tangutur AD, Khatua TN, Saxena P, Banerjee SK, Bhadra MP. A proteomic view of isoproterenol induced cardiac hypertrophy: prohibitin identified as a potential biomarker in rats. J Transl Med. 2013;11:130. Epub 2013/05/28. doi: 10.1186/1479-5876-11-130. PubMed PMID: 23706090; PMCID: PMC3667141.
31. van Heesch S, Witte F, Schneider-Lunitz V, Schulz JF, Adami E, Faber AB, Kirchner M, Maatz H, Blachut S, Sandmann CL, Kanda M, Worth CL, Schafer S, Calviello L, Merriott R, Patone G, Hummel O, Wyler E, Obermayer B, Mucke MB, Lindberg EL, Trnka F, Memczak S, Schilling M, Felkin LE, Barton PJR, Quaife NM, Vanezis K, Diecke S, Mukai M, Mah N, Oh SJ, Kurtz A, Schramm C, Schwinge D, Sebode M, Harakalova M, Asselbergs FW, Vink A, de Weger RA, Viswanathan S, Widjaja AA, Gartner-Rommel A, Milting H, Dos Remedios C, Knosalla C, Mertins P, Landthaler M, Vingron M, Linke WA, Seidman JG, Seidman CE, Rajewsky N, Ohler U, Cook SA, Hubner N. The Translational Landscape of the Human Heart. Cell. 2019;178(1):242-60 e29. Epub 2019/06/04. doi: 10.1016/j.cell.2019.05.010. PubMed PMID: 31155234.
32. Krahl ME. Incorporation of C14-amino acids into glutathione and protein fractions of normal and diabetic rat tissues. J Biol Chem. 1953;200(1):99-109. Epub 1953/01/01. PubMed PMID: 13034763.
33. Proud CG. mTORC1 regulates the efficiency and cellular capacity for protein synthesis. Biochem Soc Trans. 2013;41(4):923-6. Epub 2013/07/19. doi: 10.1042/BST20130036. PubMed PMID: 23863157.
34. Fingar DC, Richardson CJ, Tee AR, Cheatham L, Tsou C, Blenis J. mTOR controls cell cycle progression through its cell growth effectors S6K1 and 4E-BP1/eukaryotic translation initiation factor 4E. Molecular and Cellular Biology. 2004;24(1):200-16. doi: 10.1128/Mcb.24.1.200-216.2004. PubMed PMID: WOS:000187531200019.

35. Chothani S, Schafer S, Adami E, Viswanathan S, Widjaja AA, Langley SR, Tan J, Wang M, Quaife NM, Jian Pua C, D'Agostino G, Guna Shekeran S, George BL, Lim S, Yiqun Cao E, van Heesch S, Witte F, Felkin LE, Christodoulou EG, Dong J, Blachut S, Patone G, Barton PJR, Hubner N, Cook SA, Rackham OJL. Widespread Translational Control of Fibrosis in the Human Heart by RNA-Binding Proteins. Circulation. 2019;140(11):937-51. Epub 2019/07/10. doi: 10.1161/CIRCULATIONAHA.119.039596. PubMed PMID: 31284728; PMCID: PMC6749977.
36. Sanford CF, Griffin EE, Wildenthal K. Synthesis and degradation of myocardial protein during the development and regression of thyroxine-induced cardiac hypertrophy in rats. Circ Res. 1978;43(5):688-94. Epub 1978/11/01. doi: 10.1161/01.res.43.5.688. PubMed PMID: 152166.
37. Knight JRP, Garland G, Poyry T, Mead E, Vlahov N, Sfakianos A, Grosso S, De-Lima-Hedayioglu F, Mallucci GR, von der Haar T, Smales CM, Sansom OJ, Willis AE. Control of translation elongation in health and disease. Dis Model Mech. 2020;13(3). Epub 2020/04/17. doi: 10.1242/dmm.043208. PubMed PMID: 32298235; PMCID: PMC7104864.
38. Leprivier G, Remke M, Rotblat B, Dubuc A, Mateo AR, Kool M, Agnihotri S, El-Naggar A, Yu B, Somasekharan SP, Faubert B, Bridon G, Tognon CE, Mathers J, Thomas R, Li A, Barokas A, Kwok B, Bowden M, Smith S, Wu X, Korshunov A, Hielscher T, Northcott PA, Galpin JD, Ahern CA, Wang Y, McCabe MG, Collins VP, Jones RG, Pollak M, Delattre O, Gleave ME, Jan E, Pfister SM, Proud CG, Derry WB, Taylor MD, Sorensen PH. The eEF2 kinase confers resistance to nutrient deprivation by blocking translation elongation. Cell. 2013;153(5):1064-79. Epub 2013/05/28. doi: 10.1016/j.cell.2013.04.055. PubMed PMID: 23706743; PMCID: PMC4395874.
39. Kurata S, Nielsen KH, Mitchell SF, Lorsch JR, Kaji A, Kaji H. Ribosome recycling step in yeast cytoplasmic protein synthesis is catalyzed by eEF3 and ATP. Proc Natl Acad Sci U S A. 2010;107(24):10854-9. Epub 2010/06/11. doi: 10.1073/pnas.1006247107. PubMed PMID: 20534490; PMCID: PMC2890720.
40. Sogorin EA, Agalarov S, Spirin AS. Inter-polysomal coupling of termination and initiation during translation in eukaryotic cell-free system. Sci Rep. 2016;6:24518. Epub 2016/04/15. doi: 10.1038/srep24518. PubMed PMID: 27075299; PMCID: PMC4830951.
41. Khatter H, Myasnikov AG, Natchiar SK, Klaholz BP. Structure of the human 80S ribosome. Nature. 2015;520(7549):640-5. Epub 2015/04/23. doi: 10.1038/nature14427. PubMed PMID: 25901680.
42. Woolford JL, Jr., Baserga SJ. Ribosome biogenesis in the yeast Saccharomyces cerevisiae. Genetics. 2013;195(3):643-81. Epub 2013/11/06. doi: 10.1534/genetics.113.153197. PubMed PMID: 24190922; PMCID: PMC3813855.
43. Malinovskaya EM, Ershova ES, Golimbet VE, Porokhovnik LN, Lyapunova NA, Kutsev SI, Veiko NN, Kostyuk SV. Copy Number of Human Ribosomal Genes With Aging: Unchanged Mean, but Narrowed Range and Decreased Variance in Elderly Group. Front Genet. 2018;9:306. Epub 2018/08/23. doi: 10.3389/fgene.2018.00306. PubMed PMID: 30131826; PMCID: PMC6090032.
44. Haltiner MM, Smale ST, Tjian R. Two distinct promoter elements in the human rRNA gene identified by linker scanning mutagenesis. Mol Cell Biol. 1986;6(1):227-35. Epub 1986/01/01. doi: 10.1128/mcb.6.1.227. PubMed PMID: 3785147; PMCID: PMC367502.
45. Kusnadi EP, Hannan KM, Hicks RJ, Hannan RD, Pearson RB, Kang J. Regulation of rDNA transcription in response to growth factors, nutrients and energy. Gene. 2015;556(1):27-34. Epub 2014/12/03. doi: 10.1016/j.gene.2014.11.010. PubMed PMID: 25447905.

46. Hannan KM, Brandenburger Y, Jenkins A, Sharkey K, Cavanaugh A, Rothblum L, Moss T, Poortinga G, McArthur GA, Pearson RB, Hannan RD. mTOR-dependent regulation of ribosomal gene transcription requires S6K1 and is mediated by phosphorylation of the carboxy-terminal activation domain of the nucleolar transcription factor UBF. Mol Cell Biol. 2003;23(23):8862-77. Epub 2003/11/13. doi: 10.1128/mcb.23.23.8862-8877.2003. PubMed PMID: 14612424; PMCID: PMC262650.
47. Mayer C, Zhao J, Yuan X, Grummt I. mTOR-dependent activation of the transcription factor TIF-IA links rRNA synthesis to nutrient availability. Genes Dev. 2004;18(4):423-34. Epub 2004/03/09. doi: 10.1101/gad.285504. PubMed PMID: 15004009; PMCID: PMC359396.
48. Hoppe S, Bierhoff H, Cado I, Weber A, Tiebe M, Grummt I, Voit R. AMP-activated protein kinase adapts rRNA synthesis to cellular energy supply. Proc Natl Acad Sci U S A. 2009;106(42):17781-6. Epub 2009/10/10. doi: 10.1073/pnas.0909873106. PubMed PMID: 19815529; PMCID: PMC2764937.
49. Klinge S, Woolford JL, Jr. Ribosome assembly coming into focus. Nat Rev Mol Cell Biol. 2019;20(2):116-31. Epub 2018/11/24. doi: 10.1038/s41580-018-0078-y. PubMed PMID: 30467428.
50. Lykke-Andersen S, Ardal BK, Hollensen AK, Damgaard CK, Jensen TH. Box C/D snoRNP Autoregulation by a cis-Acting snoRNA in the NOP56 Pre-mRNA. Mol Cell. 2018;72(1):99-111 e5. Epub 2018/09/18. doi: 10.1016/j.molcel.2018.08.017. PubMed PMID: 30220559.
51. Miyazaki K, Yamashita T, Morimoto N, Sato K, Mimoto T, Kurata T, Ikeda Y, Abe K. Early and selective reduction of NOP56 (Asidan) and RNA processing proteins in the motor neuron of ALS model mice. Neurol Res. 2013;35(7):744-54. Epub 2013/04/16. doi: 10.1179/1743132813Y.0000000196. PubMed PMID: 23582672.
52. Lechertier T, Grob A, Hernandez-Verdun D, Roussel P. Fibrillarin and Nop56 interact before being co-assembled in box C/D snoRNPs. Exp Cell Res. 2009;315(6):928-42. Epub 2009/04/01. doi: 10.1016/j.yexcr.2009.01.016. PubMed PMID: 19331828.
53. Paul A, Tiotiu D, Bragantini B, Marty H, Charpentier B, Massenet S, Labialle S. Bcd1p controls RNA loading of the core protein Nop58 during C/D box snoRNP biogenesis. RNA. 2019;25(4):496-506. Epub 2019/02/01. doi: 10.1261/rna.067967.118. PubMed PMID: 30700579; PMCID: PMC6426285.
54. McKeegan KS, Debieux CM, Watkins NJ. Evidence that the AAA+ proteins TIP48 and TIP49 bridge interactions between 15.5K and the related NOP56 and NOP58 proteins during box C/D snoRNP biogenesis. Mol Cell Biol. 2009;29(18):4971-81. Epub 2009/07/22. doi: 10.1128/MCB.00752-09. PubMed PMID: 19620283; PMCID: PMC2738292.
55. Iyer-Bierhoff A, Krogh N, Tessarz P, Ruppert T, Nielsen H, Grummt I. SIRT7-Dependent Deacetylation of Fibrillarin Controls Histone H2A Methylation and rRNA Synthesis during the Cell Cycle. Cell Rep. 2018;25(11):2946-54 e5. Epub 2018/12/13. doi: 10.1016/j.celrep.2018.11.051. PubMed PMID: 30540930.
56. Peterson LK, Jaskowski TD, Mayes MD, Tebo AE. Detection of anti-U3-RNP/fibrillarin IgG antibodies by line immunoblot assay has comparable clinical significance to immunoprecipitation testing in systemic sclerosis. Immunol Res. 2016;64(2):483-8. Epub 2015/10/16. doi: 10.1007/s12026-015-8710-9. PubMed PMID: 26467972.
57. Fatica A, Galardi S, Altieri F, Bozzoni I. Fibrillarin binds directly and specifically to U16 box C/D snoRNA. RNA. 2000;6(1):88-95. Epub 2000/02/11. doi: 10.1017/s1355838200991623. PubMed PMID: 10668801; PMCID: PMC1369896.

58. Cavaille J, Bachellerie JP. Processing of fibrillarin-associated snoRNAs from pre-mRNA introns: an exonucleolytic process exclusively directed by the common stem-box terminal structure. Biochimie. 1996;78(6):443-56. Epub 1996/01/01. doi: 10.1016/0300-9084(96)84751-1. PubMed PMID: 8915534.
59. Ghisolfi-Nieto L, Joseph G, Puvion-Dutilleul F, Amalric F, Bouvet P. Nucleolin is a sequence-specific RNA-binding protein: characterization of targets on pre-ribosomal RNA. J Mol Biol. 1996;260(1):34-53. Epub 1996/07/05. doi: 10.1006/jmbi.1996.0380. PubMed PMID: 8676391.
60. Cong R, Das S, Ugrinova I, Kumar S, Mongelard F, Wong J, Bouvet P. Interaction of nucleolin with ribosomal RNA genes and its role in RNA polymerase I transcription. Nucleic Acids Res. 2012;40(19):9441-54. Epub 2012/08/04. doi: 10.1093/nar/gks720. PubMed PMID: 22859736; PMCID: PMC3479187.
61. Rees-Unwin KS, Faragher R, Unwin RD, Adams J, Brown PJ, Buckle AM, Pettitt A, Hutchinson CV, Johnson SM, Pulford K, Banham AH, Whetton AD, Lucas G, Mason DY, Burthem J. Ribosome-associated nucleophosmin 1: increased expression and shuttling activity distinguishes prognostic subtypes in chronic lymphocytic leukaemia. Br J Haematol. 2010;148(4):534-43. Epub 2009/12/08. doi: 10.1111/j.1365-2141.2009.07979.x. PubMed PMID: 19961478.
62. Okuwaki M, Tsujimoto M, Nagata K. The RNA binding activity of a ribosome biogenesis factor, nucleophosmin/B23, is modulated by phosphorylation with a cell cycle-dependent kinase and by association with its subtype. Mol Biol Cell. 2002;13(6):2016-30. Epub 2002/06/12. doi: 10.1091/mbc.02-03-0036. PubMed PMID: 12058066; PMCID: PMC117621.
63. Morello LG, Hesling C, Coltri PP, Castilho BA, Rimokh R, Zanchin NI. The NIP7 protein is required for accurate pre-rRNA processing in human cells. Nucleic Acids Res. 2011;39(2):648-65. Epub 2010/08/28. doi: 10.1093/nar/gkq758. PubMed PMID: 20798176; PMCID: PMC3025556.
64. Morello LG, Coltri PP, Quaresma AJ, Simabuco FM, Silva TC, Singh G, Nickerson JA, Oliveira CC, Moore MJ, Zanchin NI. The human nucleolar protein FTSJ3 associates with NIP7 and functions in pre-rRNA processing. PLoS One. 2011;6(12):e29174. Epub 2011/12/24. doi: 10.1371/journal.pone.0029174. PubMed PMID: 22195017; PMCID: PMC3241699.
65. Strezoska Z, Pestov DG, Lau LF. Bop1 is a mouse WD40 repeat nucleolar protein involved in 28S and 5. 8S RRNA processing and 60S ribosome biogenesis. Mol Cell Biol. 2000;20(15):5516-28. Epub 2000/07/13. doi: 10.1128/mcb.20.15.5516-5528.2000. PubMed PMID: 10891491; PMCID: PMC86002.
66. Pestov DG, Strezoska Z, Lau LF. Evidence of p53-dependent cross-talk between ribosome biogenesis and the cell cycle: effects of nucleolar protein Bop1 on G(1)/S transition. Mol Cell Biol. 2001;21(13):4246-55. Epub 2001/06/08. doi: 10.1128/MCB.21.13.4246-4255.2001. PubMed PMID: 11390653; PMCID: PMC87085.
67. Chu YD, Chen HK, Huang T, Chan SP. A novel function for the DEAD-box RNA helicase DDX-23 in primary microRNA processing in Caenorhabditis elegans. Dev Biol. 2016;409(2):459-72. Epub 2015/11/26. doi: 10.1016/j.ydbio.2015.11.011. PubMed PMID: 26601717.
68. Abdelhaleem M, Maltais L, Wain H. The human DDX and DHX gene families of putative RNA helicases. Genomics. 2003;81(6):618-22. Epub 2003/06/05. doi: 10.1016/s0888-7543(03)00049-1. PubMed PMID: 12782131.

69. Grote P, Wittler L, Hendrix D, Koch F, Wahrisch S, Beisaw A, Macura K, Blass G, Kellis M, Werber M, Herrmann BG. The tissue-specific lncRNA Fendrr is an essential regulator of heart and body wall development in the mouse. Dev Cell. 2013;24(2):206-14. Epub 2013/02/02. doi: 10.1016/j.devcel.2012.12.012. PubMed PMID: 23369715; PMCID: PMC4149175.
70. Hou J, Long H, Zhou C, Zheng S, Wu H, Guo T, Wu Q, Zhong T, Wang T. Long noncoding RNA Braveheart promotes cardiogenic differentiation of mesenchymal stem cells in vitro. Stem Cell Res Ther. 2017;8(1):4. Epub 2017/01/18. doi: 10.1186/s13287-016-0454-5. PubMed PMID: 28095922; PMCID: PMC5242041.
71. Han P, Li W, Lin CH, Yang J, Shang C, Nuernberg ST, Jin KK, Xu W, Lin CY, Lin CJ, Xiong Y, Chien H, Zhou B, Ashley E, Bernstein D, Chen PS, Chen HV, Quertermous T, Chang CP. A long noncoding RNA protects the heart from pathological hypertrophy. Nature. 2014;514(7520):102-6. Epub 2014/08/15. doi: 10.1038/nature13596. PubMed PMID: 25119045; PMCID: PMC4184960.
72. Viereck J, Kumarswamy R, Foinquinos A, Xiao K, Avramopoulos P, Kunz M, Dittrich M, Maetzig T, Zimmer K, Remke J, Just A, Fendrich J, Scherf K, Bolesani E, Schambach A, Weidemann F, Zweigerdt R, de Windt LJ, Engelhardt S, Dandekar T, Batkai S, Thum T. Long noncoding RNA Chast promotes cardiac remodeling. Sci Transl Med. 2016;8(326):326ra22. Epub 2016/02/19. doi: 10.1126/scitranslmed.aaf1475. PubMed PMID: 26888430.
73. Wang Z, Zhang XJ, Ji YX, Zhang P, Deng KQ, Gong J, Ren S, Wang X, Chen I, Wang H, Gao C, Yokota T, Ang YS, Li S, Cass A, Vondriska TM, Li G, Deb A, Srivastava D, Yang HT, Xiao X, Li H, Wang Y. The long noncoding RNA Chaer defines an epigenetic checkpoint in cardiac hypertrophy. Nat Med. 2016;22(10):1131-9. Epub 2016/09/13. doi: 10.1038/nm.4179. PubMed PMID: 27618650; PMCID: PMC5053883.
74. Ishii N, Ozaki K, Sato H, Mizuno H, Susumu S, Takahashi A, Miyamoto Y, Ikegawa S, Kamatani N, Hori M, Satoshi S, Nakamura Y, Tanaka T. Identification of a novel non-coding RNA, MIAT, that confers risk of myocardial infarction. J Hum Genet. 2006;51(12):1087-99. Epub 2006/10/27. doi: 10.1007/s10038-006-0070-9. PubMed PMID: 17066261.
75. Rao SQ, Hu HL, Ye N, Shen Y, Xu Q. Genetic variants in long non-coding RNA MIAT contribute to risk of paranoid schizophrenia in a Chinese Han population. Schizophr Res. 2015;166(1-3):125-30. Epub 2015/05/26. doi: 10.1016/j.schres.2015.04.032. PubMed PMID: 26004688.
76. Wang XM, Li XM, Song N, Zhai H, Gao XM, Yang YN. Long non-coding RNAs H19, MALAT1 and MIAT as potential novel biomarkers for diagnosis of acute myocardial infarction. Biomed Pharmacother. 2019;118:109208. Epub 2019/07/16. doi: 10.1016/j.biopha.2019.109208. PubMed PMID: 31302423.
77. Yan B, Yao J, Liu JY, Li XM, Wang XQ, Li YJ, Tao ZF, Song YC, Chen Q, Jiang Q. lncRNA-MIAT regulates microvascular dysfunction by functioning as a competing endogenous RNA. Circ Res. 2015;116(7):1143-56. Epub 2015/01/15. doi: 10.1161/CIRCRESAHA.116.305510. PubMed PMID: 25587098.
78. Deng W, Fan C, Shen R, Wu Y, Du R, Teng J. Long noncoding MIAT acting as a ceRNA to sponge microRNA-204-5p to participate in cerebral microvascular endothelial cell injury after cerebral ischemia through regulating HMGB1. J Cell Physiol. 2020;235(5):4571-86. Epub 2019/10/20. doi: 10.1002/jcp.29334. PubMed PMID: 31628679.
79. Zhou L, Xu DY, Sha WG, Shen L, Lu GY, Yin X. Long non-coding MIAT mediates high glucose-induced renal tubular epithelial injury. Biochem Biophys Res Commun.

2015;468(4):726-32. Epub 2015/11/10. doi: 10.1016/j.bbrc.2015.11.023. PubMed PMID: 26551455.
80. Sattari A, Siddiqui H, Moshiri F, Ngankeu A, Nakamura T, Kipps TJ, Croce CM. Upregulation of long noncoding RNA MIAT in aggressive form of chronic lymphocytic leukemias. Oncotarget. 2016;7(34):54174-82. Epub 2016/08/17. doi: 10.18632/oncotarget.11099. PubMed PMID: 27527866; PMCID: PMC5338916.
81. Lai IL, Yang CA, Lin PC, Chan WL, Lee YT, Yen JC, Chang YS, Chang JG. Long noncoding RNA MIAT promotes non-small cell lung cancer proliferation and metastasis through MMP9 activation. Oncotarget. 2017;8(58):98148-62. Epub 2017/12/13. doi: 10.18632/oncotarget.21465. PubMed PMID: 29228680; PMCID: PMC5716720.
82. Zhang HY, Zheng FS, Yang W, Lu JB. The long non-coding RNA MIAT regulates zinc finger E-box binding homeobox 1 expression by sponging miR-150 and promoteing cell invasion in non-small-cell lung cancer. Gene. 2017;633:61-5. Epub 2017/08/28. doi: 10.1016/j.gene.2017.08.009. PubMed PMID: 28843520.
83. Jiang Q, Shan K, Qun-Wang X, Zhou RM, Yang H, Liu C, Li YJ, Yao J, Li XM, Shen Y, Cheng H, Yuan J, Zhang YY, Yan B. Long non-coding RNA-MIAT promotes neurovascular remodeling in the eye and brain. Oncotarget. 2016;7(31):49688-98. Epub 2016/07/09. doi: 10.18632/oncotarget.10434. PubMed PMID: 27391072; PMCID: PMC5226539.
84. Qu X, Du Y, Shu Y, Gao M, Sun F, Luo S, Yang T, Zhan L, Yuan Y, Chu W, Pan Z, Wang Z, Yang B, Lu Y. MIAT Is a Pro-fibrotic Long Non-coding RNA Governing Cardiac Fibrosis in Post-infarct Myocardium. Sci Rep. 2017;7:42657. Epub 2017/02/16. doi: 10.1038/srep42657. PubMed PMID: 28198439; PMCID: PMC5309829.
85. Li Y, Wang J, Sun L, Zhu S. LncRNA myocardial infarction-associated transcript (MIAT) contributed to cardiac hypertrophy by regulating TLR4 via miR-93. Eur J Pharmacol. 2018;818:508-17. Epub 2017/11/22. doi: 10.1016/j.ejphar.2017.11.031. PubMed PMID: 29157986.
86. Tan J, Liu S, Jiang Q, Yu T, Huang K. LncRNA-MIAT Increased in Patients with Coronary Atherosclerotic Heart Disease. Cardiol Res Pract. 2019;2019:6280194. Epub 2019/05/31. doi: 10.1155/2019/6280194. PubMed PMID: 31143478; PMCID: PMC6501139.
87. Chen L, Zhang D, Yu L, Dong H. Targeting MIAT reduces apoptosis of cardiomyocytes after ischemia/reperfusion injury. Bioengineered. 2019;10(1):121-32. Epub 2019/04/12. doi: 10.1080/21655979.2019.1605812. PubMed PMID: 30971184; PMCID: PMC6527071.
88. Cong L, Su Y, Wei D, Qian L, Xing D, Pan J, Chen Y, Huang M. Catechin relieves hypoxia/reoxygenation-induced myocardial cell apoptosis via down-regulating lncRNA MIAT. J Cell Mol Med. 2020;24(3):2356-68. Epub 2020/01/20. doi: 10.1111/jcmm.14919. PubMed PMID: 31955523; PMCID: PMC7011153.
89. Ghazalpour A, Rau CD, Farber CR, Bennett BJ, Orozco LD, van Nas A, Pan C, Allayee H, Beaven SW, Civelek M, Davis RC, Drake TA, Friedman RA, Furlotte N, Hui ST, Jentsch JD, Kostem E, Kang HM, Kang EY, Joo JW, Korshunov VA, Laughlin RE, Martin LJ, Ohmen JD, Parks BW, Pellegrini M, Reue K, Smith DJ, Tetradis S, Wang J, Wang Y, Weiss JN, Kirchgessner T, Gargalovic PS, Eskin E, Lusis AJ, LeBoeuf RC. Hybrid mouse diversity panel: a panel of inbred mouse strains suitable for analysis of complex genetic traits. Mamm Genome. 2012;23(9-10):680-92. Epub 2012/08/16. doi: 10.1007/s00335-012-9411-5. PubMed PMID: 22892838; PMCID: PMC3586763.
90. Lusis AJ, Seldin MM, Allayee H, Bennett BJ, Civelek M, Davis RC, Eskin E, Farber CR, Hui S, Mehrabian M, Norheim F, Pan C, Parks B, Rau CD, Smith DJ, Vallim T, Wang Y, Wang

J. The Hybrid Mouse Diversity Panel: a resource for systems genetics analyses of metabolic and cardiovascular traits. J Lipid Res. 2016;57(6):925-42. Epub 2016/04/22. doi: 10.1194/jlr.R066944. PubMed PMID: 27099397; PMCID: PMC4878195.
91. Lee JH, Gao C, Peng G, Greer C, Ren S, Wang Y, Xiao X. Analysis of transcriptome complexity through RNA sequencing in normal and failing murine hearts. Circ Res. 2011;109(12):1332-41. Epub 2011/10/29. doi: 10.1161/CIRCRESAHA.111.249433. PubMed PMID: 22034492; PMCID: PMC3243366.
92. Warner JR, Vilardell J, Sohn JH. Economics of ribosome biosynthesis. Cold Spring Harb Symp Quant Biol. 2001;66:567-74. Epub 2003/05/24. PubMed PMID: 12762058.
93. Granneman S, Baserga SJ. Ribosome biogenesis: of knobs and RNA processing. Exp Cell Res. 2004;296(1):43-50. Epub 2004/05/04. doi: 10.1016/j.yexcr.2004.03.016. PubMed PMID: 15120992.
94. Nazar RN. Ribosomal RNA processing and ribosome biogenesis in eukaryotes. IUBMB Life. 2004;56(8):457-65. Epub 2004/11/17. doi: 10.1080/15216540400010867. PubMed PMID: 15545225.
95. Sanghai ZA, Miller L, Molloy KR, Barandun J, Hunziker M, Chaker-Margot M, Wang J, Chait BT, Klinge S. Modular assembly of the nucleolar pre-60S ribosomal subunit. Nature. 2018;556(7699):126-9. doi: 10.1038/nature26156. PubMed PMID: 29512650; PMCID: PMC6118127.
96. Montacie C, Durut N, Opsomer A, Palm D, Comella P, Picart C, Carpentier MC, Pontvianne F, Carapito C, Schleiff E, Saez-Vasquez J. Nucleolar Proteome Analysis and Proteasomal Activity Assays Reveal a Link between Nucleolus and 26S Proteasome in A. thaliana. Front Plant Sci. 2017;8:1815. Epub 2017/11/07. doi: 10.3389/fpls.2017.01815. PubMed PMID: 29104584; PMCID: PMC5655116.
97. Moreira D, Ranjard L, Lopez-Garcia P. The nucleolar proteome and the (endosymbiotic) origin of the nucleus. Bioessays. 2004;26(10):1144-5; author reply 5-7. Epub 2004/09/24. doi: 10.1002/bies.20122. PubMed PMID: 15382131.
98. Coute Y, Burgess JA, Diaz JJ, Chichester C, Lisacek F, Greco A, Sanchez JC. Deciphering the human nucleolar proteome. Mass Spectrom Rev. 2006;25(2):215-34. Epub 2005/10/08. doi: 10.1002/mas.20067. PubMed PMID: 16211575.
99. Avitabile D, Bailey B, Cottage CT, Sundararaman B, Joyo A, McGregor M, Gude N, Truffa S, Zarrabi A, Konstandin M, Khan M, Mohsin S, Volkers M, Toko H, Mason M, Cheng Z, Din S, Alvarez R, Jr., Fischer K, Sussman MA. Nucleolar stress is an early response to myocardial damage involving nucleolar proteins nucleostemin and nucleophosmin. Proc Natl Acad Sci U S A. 2011;108(15):6145-50. doi: 10.1073/pnas.1017935108. PubMed PMID: 21444791; PMCID: PMC3076816.
100. Rosello-Lleti E, Rivera M, Cortes R, Azorin I, Sirera R, Martinez-Dolz L, Hove L, Cinca J, Lago F, Gonzalez-Juanatey JR, Salvador A, Portoles M. Influence of heart failure on nucleolar organization and protein expression in human hearts. Biochem Biophys Res Commun. 2012;418(2):222-8. Epub 2012/01/17. doi: 10.1016/j.bbrc.2011.12.151. PubMed PMID: 22244875.
101. Matos-Perdomo E, Machin F. TORC1, stress and the nucleolus. Aging (Albany NY). 2018;10(5):857-8. Epub 2018/05/23. doi: 10.18632/aging.101456. PubMed PMID: 29788001; PMCID: PMC5990385.

102. Boulon S, Westman BJ, Hutten S, Boisvert FM, Lamond AI. The nucleolus under stress. Mol Cell. 2010;40(2):216-27. Epub 2010/10/23. doi: 10.1016/j.molcel.2010.09.024. PubMed PMID: 20965417; PMCID: PMC2987465.
103. Serin G, Joseph G, Faucher C, Ghisolfi L, Bouche G, Amalric F, Bouvet P. Localization of nucleolin binding sites on human and mouse pre-ribosomal RNA. Biochimie. 1996;78(6):530-8. Epub 1996/01/01. PubMed PMID: 8915542.
104. Perry RB, Rishal I, Doron-Mandel E, Kalinski AL, Medzihradszky KF, Terenzio M, Alber S, Koley S, Lin A, Rozenbaum M, Yudin D, Sahoo PK, Gomes C, Shinder V, Geraisy W, Huebner EA, Woolf CJ, Yaron A, Burlingame AL, Twiss JL, Fainzilber M. Nucleolin-Mediated RNA Localization Regulates Neuron Growth and Cycling Cell Size. Cell Rep. 2016;16(6):1664-76. Epub 2016/08/02. doi: 10.1016/j.celrep.2016.07.005. PubMed PMID: 27477284; PMCID: PMC4978702.
105. Wang KK, Jiang L, E SM, Liu K, Zhang LL, Liu MD, Xiao XZ. [Effect of nucleolin down-regulation on the proliferation and apoptosis in C2C12 cells]. Zhong Nan Da Xue Xue Bao Yi Xue Ban. 2005;30(2):125-9. Epub 2005/05/19. PubMed PMID: 15898417.
106. Jiang B, Zhang B, Liang P, Chen G, Zhou B, Lv C, Tu Z, Xiao X. Nucleolin protects the heart from ischaemia-reperfusion injury by up-regulating heat shock protein 32. Cardiovasc Res. 2013;99(1):92-101. Epub 2013/04/19. doi: 10.1093/cvr/cvt085. PubMed PMID: 23594402.
107. Qin Z, Lavingia B, Zou Y, Stastny P. Antibodies against nucleolin in recipients of organ transplants. Transplantation. 2011;92(7):829-35. Epub 2011/08/27. doi: 10.1097/TP.0b013e31822d0977. PubMed PMID: 21869741.
108. Christian S, Pilch J, Akerman ME, Porkka K, Laakkonen P, Ruoslahti E. Nucleolin expressed at the cell surface is a marker of endothelial cells in angiogenic blood vessels. J Cell Biol. 2003;163(4):871-8. Epub 2003/11/26. doi: 10.1083/jcb.200304132. PubMed PMID: 14638862; PMCID: PMC2173679.
109. Borer RA, Lehner CF, Eppenberger HM, Nigg EA. Major nucleolar proteins shuttle between nucleus and cytoplasm. Cell. 1989;56(3):379-90. Epub 1989/02/10. doi: 10.1016/0092-8674(89)90241-9. PubMed PMID: 2914325.
110. Schmidt EK, Clavarino G, Ceppi M, Pierre P. SUnSET, a nonradioactive method to monitor protein synthesis. Nat Methods. 2009;6(4):275-7. Epub 2009/03/24. doi: 10.1038/nmeth.1314. PubMed PMID: 19305406.
111. Esposito AM, Mateyak M, He D, Lewis M, Sasikumar AN, Hutton J, Copeland PR, Kinzy TG. Eukaryotic polyribosome profile analysis. J Vis Exp. 2010(40). Epub 2010/06/23. doi: 10.3791/1948. PubMed PMID: 20567211; PMCID: PMC3149985.